NRL REPORT E-3482

ER-3482

A MAGNETIC AMPLIFIER CONTROL UNIT FOR CONSTANT FREQUENCY

NAVAL RESEARCH LABORATORY

WASHINGTON, D.C.

NRL REPORT E-3482

A MAGNETIC AMPLIFIER CONTROL UNIT FOR CONSTANT FREQUENCY

H. G. Schafer and L. J. Johnson

June 27, 1949

Approved by:

Mr. W. B. Roberts, Head, Interior Communications Branch
Dr. Wayne C. Hall, Superintendent, Electricity Division

NAVAL RESEARCH LABORATORY
CAPTAIN F. R. FURTH, USN, DIRECTOR
WASHINGTON, D.C.

DISTRIBUTION

BuShips	
Attn: Code 330	5
Attn: Code 665	50
Attn: Code 660	2
Attn: Code 345	2
BuOrd	
Attn: Code Re4a	2
Attn: Code REC-3	2
BuAer	
Attn: Code TD-4	2
CNO	1
CDR., New York Naval Shipyard	
Attn: Material Lab.	2
Dir., USNEL	2
CDR., USNOTS	
Attn: Reports Unit	2
Dir., USNEES	2
OCSigO	
Attn: Ch. Eng. & Tech. Div., SIGTM-S	1
CO, SCEL	
Attn: Dir. of Engineering	2
CG, AMC, Wright-Patterson Air Force Base	
Attn: Section MCREXE-13	2
Attn: Eng. Div., Electronics Subdiv., MCREEO-2	1
CO, Watson Labs., AMC, Red Bank	
Attn: Air Force Cambridge Res. Labs. ENR	1
CO, Cambridge	
Attn: ERRS	1
BAGR, CD, Wright-Patterson Air Force Base	
Attn: CADO-D1	1
CO, NADS, Johnsville	2
RDB	
Attn: Library	2
Attn: Navy Secretary	1
Naval Research Sec. of the Science Div., Lib. of Congress	
Attn: Mr. J. H. Heald	2

CONTENTS

ABSTRACT

In line with a program for improving underwater log systems, a development problem for an improved constant-frequency control system was authorized. A control unit, in the form of a magnetic servo-amplifier and two resonant frequency-sensing circuits controlling the frequency of a rotary inverter, is described as a solution to the problem.

The performance requirements of a suitable control system, design details of the system and its components, and final performance data of a working model, are presented and discussed. It is shown that a frequency control without moving parts can be designed to maintain the frequency of an inverter to a tolerance of ±0.1 percent, under conditions of variable supply voltage, loads, and temperatures. Test results are submitted to show the extent to which the final model was subjected to service conditions.

Among the circuit and component design considerations, those concerned with saturable reactors and anti-hunt or damping methods may have general applications to frequency controls and servo systems.

PROBLEM STATUS

This is a final report on the problem. Unless the Laboratory is otherwise advised by the Bureau, the problem will be closed one month from the mailing date of this report.

AUTHORIZATION

NRL Problem E04-04D
(BuShips ltr S65-5(335C), March 5, 1946

A MAGNETIC AMPLIFIER CONTROL UNIT FOR CONSTANT FREQUENCY

INTRODUCTION

Many electrical measuring devices on shipboard require a constant-frequency alternating-current power source for their operation. For most purposes, the frequency regulation of a shipboard power source is not critical and may therefore be permitted to vary a few cycles per second above or below its nominal 60-cycle frequency. However, when the frequency of the power supply is used as a standard time reference (as it is in some log systems, shaft-revolution indicators, and dead-reckoning plotters) the frequency must be held to a tolerance of 0.1 percent or better. Usually, only a relatively small amount of power of closely regulated frequency is required for shipboard interior-communications instruments; therefore it is general practice to supply this power from a small inverter or dynamotor running on the ship's 115-volt direct-current system. The frequency of this inverter is regulated by shunt-field current control through some type of frequency-regulator unit.

A number of methods are (or have been) in use to regulate automatically the motor field of an inverter. Most of these devices are in the form of electromechanical servo systems. The present types of electromechanical regulators are objectionable because they utilize tuning forks, vacuum tubes, and moving mechanical parts; because they are inherently sluggish in operation; and because they can be damaged by shock and vibration.

Authorization for the development project with which this report is concerned set forth the electrical specifications to be met in a proposed magnetic-amplifier frequency-control system. The performance requirements were as follows:

(a) Output of Dynamotor: 0 to 80 watts at 80 to 100-percent power factor.

(b) Output Frequency of Dynamotor: 60 cycles per second, ±0.1 percent.

(c) Output Voltage (ac) 115 volts, single phase, with no automatic voltage regulator.

(d) Power-Supply Voltage: 115 volts dc ±5 percent, or a d-c voltage ranging from 109.25 to 120.75 volts.

(e) Frequency Control: To be obtained by shunt-field control on the motor field of the dynamotor.

(f) Ambient Temperature Range: 40° to 130°F.

In order to arrive at a definite solution to this problem, it was necessary at the outset to make several decisions regarding the type of frequency regulator required and the simplest, most straightforward way of designing and developing such a regulator. Among the most important of these decisions were the following:

(a) A magnetic-amplifier circuit would be designed with no moving parts.

(b) Because of the small size of the machine to be controlled, the magnetic-amplifier efficiency would be made high in order to draw as little power as possible from the a-c output of the dynamotor unit.

(c) The shunt field of the dynamotor would be redesigned to reduce the power required for field control. An auxiliary control field and a fixed shunt field would be used in order to minimize the power drawn from the regulator circuit.

(d) The frequency-sensitive elements of the system would consist of two series-resonant circuits with rectifiers. These circuits would supply direct current to the control windings of two saturable reactors, and the reactors, in turn, would regulate the flow of power to the control-field rectifier.

(e) The cores for the saturable reactors would be made from a readily available material if possible.

(f) The use of temperature-control ovens and thermostats to maintain component stability in the system would be avoided if at all practicable.

It was learned experimentally that some modifications of these design conditions were necessary.

Technical information on magnetic amplifiers and their applications was obtained from many sources, some of which are listed in the Bibliography. However, early in the course of the investigation it was discovered that very little usable design data are available in the literature. Since the design of magnetic amplifiers is as much an art as a science, much information must be acquired by personal experience with the circuits and techniques involved. For this reason alone, considerable time was spent in learning theory and methods perhaps previously known.

In pursuing this development, the problem resolved itself into the following phases:

(a) Derivation of useful working formulas and graphical design data for saturable reactors and resonant circuits;

(b) Determination of the operating characteristics of the dynamotor for which the control system was to be designed;

(c) Design of a suitable frequency-control circuit;

(d) Construction of cores and windings; and

(e) Performance tests on various amplifier models to determine the effects of temperature, voltage, load, and power factor on the system and its components.

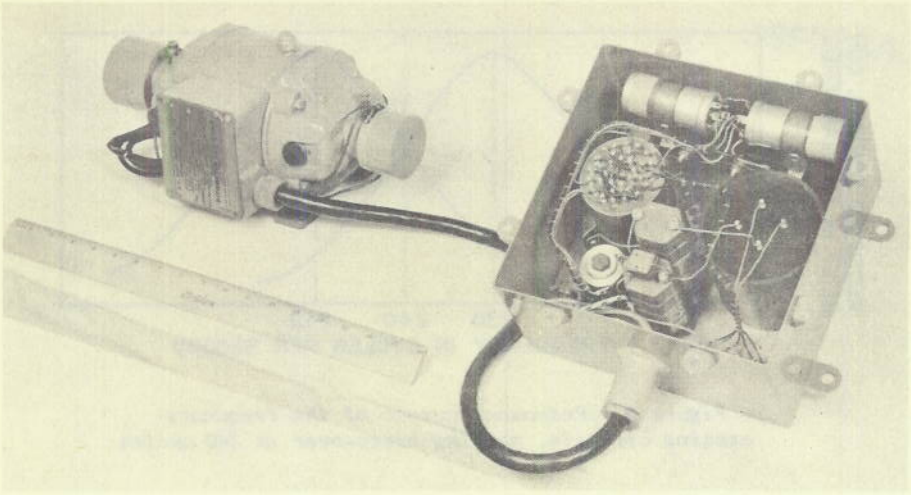

Figure 1 - Assembled magnetic amplifier frequency-control unit and dynamotor

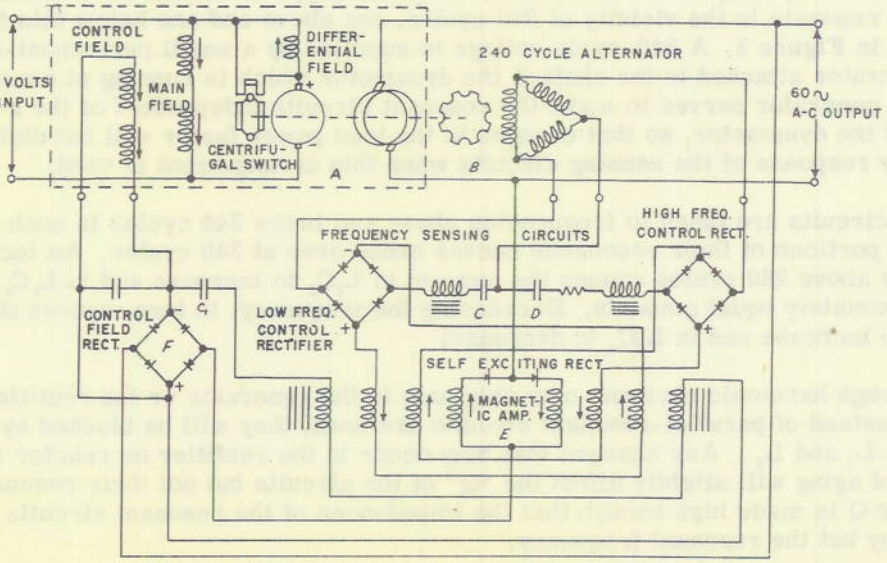

Figure 2 - Schematic diagram of the 60-cycle constant-frequency control unit

DESCRIPTION OF A SATISFACTORY CONTROL UNIT

Several versions of a frequency-control circuit were devised and tested, and many features were discarded for one reason or another. The model finally adopted is shown in its assembled form in Figure 1, and Figure 2 presents the circuit diagram for the complete unit. The circuit is essentially that of an electromechanical servo-mechanism loop, in which the output speed of the dynamotor is used to regulate the frequency of the same dynamotor through shunt-field control. The various components of the circuit fall conveniently into three main groups, namely, the frequency-sensing circuits, the magnetic amplifier, and the anti-hunt or transient-feedback circuit.

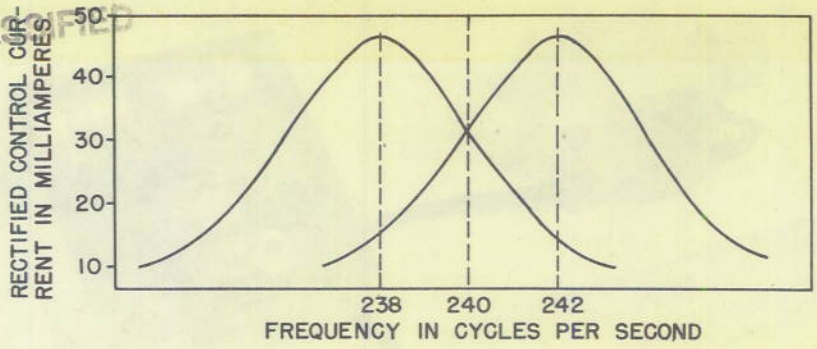

Figure 3 - Resonance curves of the frequency-sensing circuits, showing cross-over at 240 cycles

The Frequency-Sensing Circuits

The two frequency-sensing circuits, L_1C_1 and L_2C_2, are connected in series and designed to resonate in the vicinity of 240 cycles, one above and one below this frequency, as shown in Figure 3. A 240-cycle voltage is supplied by a small permanent-magnet a-c pilot generator attached to the shaft of the dynamotor which is running at exactly 60 cps. The pilot generator serves to make the resonant circuits independent of the a-c output circuit of the dynamotor, so that changes in the load power factor will not disturb the frequency response of the sensing circuits when this arrangement is used.

The circuits are tuned to frequencies above and below 240 cycles in such a way that the steep portions of their resonance curves cross over at 240 cycles. An increase in frequency above 240 cycles causes the current in L_2C_2 to increase and in L_1C_1 to decrease by approximately equal amounts. Decreasing the frequency, in turn, causes the current in L_1C_1 to increase and in L_2C_2 to decrease.

Although harmonic currents may originate in the generator or the rectifiers when series- instead of parallel-resonant circuits are used, they will be blocked by the high-Q reactors, L_1 and L_2. Any changes that may occur in the rectifier or reactor resistance because of aging will slightly affect the "Q" of the circuits but not their resonant frequencies. The Q is made high enough that the impedances of the resonant circuits are extremely high at any but the resonant frequency.

The Magnetic Amplifier

The outputs of the two frequency-sensing circuits are rectified and fed into a magnetic amplifier which regulates and feeds a portion of the 60-cycle a-c power from the dynamotor output into a control-field or main rectifier, and this rectifier supplies current to an auxiliary speed-control field winding on the motor side of the dynamotor. The magnetic amplifier consists of two toroidal reactors having four windings each and two half-wave disc rectifiers connected as shown in Figure 2. The a-c windings are in series with the control-field rectifier, one set being connected in series across the rectifier of the low-frequency tuned circuit, while the other is connected to the high-frequency tuned circuit. The magnetic fluxes induced by the windings in each of the two saturable reactors are indicated by arrows in Figure 2.

The magnetomotive forces induced in the magnetic amplifier by currents from the resonant circuits are equal and opposite when the two resonant circuits are operating at 240 cycles. Operation of the sensing circuits in combination with the magnetic amplifier can be shown, for example, by assuming an increase in the dynamotor speed due to some external disturbance. This disturbance will cause the current in control windings of the magnetic amplifier to become unbalanced, a matter which results in a magnetomotive force which aids the self-biasing of the amplifier. This action will cause the reactance of the a-c windings to be reduced. More current will flow through the a-c power windings of the amplifier, and this current increase will be passed along through the control rectifier to the control field of the dynamotor. The speed of the machine will then drop back to normal.

If, on the other hand, there should be a drop in the speed of the dynamotor, the unbalance in control current will result in a decrease in the bias of the amplifier and an increase in the reactance of the a-c windings. The current in the a-c windings will decrease, and the speed of the dynamotor will increase to its normal value once more.

The magnetic amplifier used in this system is known as the self-excited, or self-saturating doubler type. In the circuit of Figure 2, a parallel combination of saturable reactors and half-wave rectifiers is used to control the current to a load, which, in this case, is the field rectifier. The two half-wave rectifiers are conducting on alternate half-cycles, and they introduce a series of unidirectional pulses into a-c windings of each reactor alternately. These d-c pulses have a self-biasing effect on the reactors, and they effectively produce a more sharply defined bend in the saturation curve of the core material, as well as a steeper initial slope in the curve. In the presence of this self-excitation, a small additional d-c flux induced by the control windings will be sufficient to give sensitive control.

Figure 4 illustrates the operation of the saturable reactors of Figure 2. In Figure 4a, a graph is shown of magnetic flux versus direct magnetizing ampere turns for one of a pair of saturable reactors. The shape of this curve depends upon the nature and treatment of the core materials used. Two operating points are shown at (1) and (2) determined by the magnitude of the d-c flux induced by the sum of the control and self-excitation ampere turns. It may be noted that Figure 4a is a curve of flux versus magnetizing force; Figures 4b and 4c are curves of voltages. However, voltage is equivalent to rate of flux change. By using this relationship, voltages and currents can be plotted using the saturation curve of Figure 4a.

Assume, for example, that a small a-c voltage is impressed across the circuit of Figure 4d. This voltage causes a small a-c magnetizing current to flow through the half-wave rectifier in series with the reactor. The resultant d-c pulses cause the operating point to shift from 0 to a point, (1), in Figure 4a. Assume that no current flows into the control winding. At this point, the counter-emf is as shown in Figure 4b, and the resulting current is shown in Figure 4e. The reactor is not saturated in this case, and it therefore limits the ac in the circuit as would any ordinary reactor.

Assume, now, that the impressed a-c voltage is raised to a value that will cause enough self-excitation current pulses to move the operating point slightly below point (2) in Figure 4a. At this point the reactor will generate a counter-emf as shown in Figure 4c, because the positive excursions of the impressed voltage drive the core beyond saturation. When the core saturates, little or no counter-emf can be generated, and during these saturation intervals, the impressed voltage causes current flow as shown in Figure 4e. The amplitude of these current peaks for any given impressed voltage depends upon the position of operating point (2) as determined by the d-c control current and self-excitation current.

Thus it can be shown that the sensitivity of the system to small current changes in the control windings depends upon how closely the operating point can be located near the knee of the saturation curve of the reactor cores. It follows that a sharp, well-defined knee in the saturation curve is essential for sensitive control and that minimum distortion in the output-current wave form occurs when the bend in the saturation curve is 90 degrees. Core material having a rectangular hysteresis loop would be ideal material for saturable reactors, provided the area of the hysteresis loop is small.

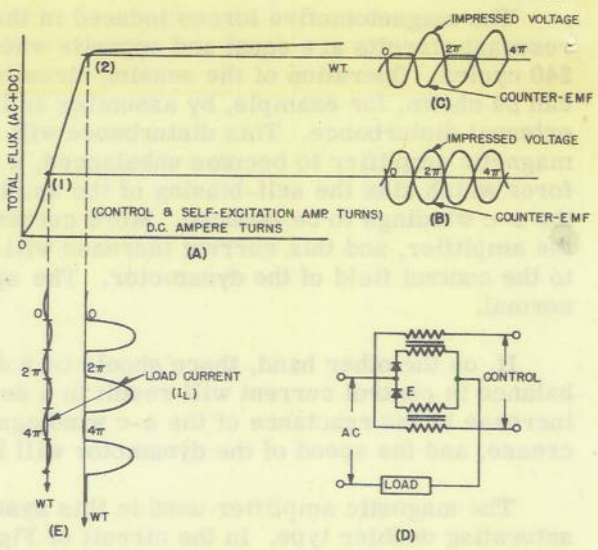

Figure 4 - Effect of saturation in the operation of a magnetic amplifier

The Transient-Feedback Circuit

The anti-hunt or transient-feedback circuit is an important part of the servo system. It consists of a large capicator and the two windings shown in Figure 2 - components which form a series circuit operating in parallel with the control-field rectifier. The condenser contains stored energy during steady-state operation, and it either dissipates some of the stored energy or absorbs more energy in such a way as to boost the correcting action of the control windings.

Such a device makes possible the use of sensitive, fast-responding circuits not otherwise applicable for reasons of instability. The period of the anti-hunt circuit is less than that of the magnetic amplifier, sensing circuits, and dynamotor in combination. Hence, the anti-hunt feature enables the system to react to any disturbance more rapidly, and thus high sensitivity is attained without loss of stability. The corrective action of the anti-hunt circuit is proportional to the rate of change of voltage across the field rectifier. Consequently, the anti-hunt circuit is an error-rate sensing device, while the resonant circuits are absolute-error sensing units.

To illustrate the action of the transient-feedback circuit, assume that a sudden drop in line voltage occurs when the system is operating. The function of the complete frequency-regulator system is to correct for such a disturbance, but it will over-correct and cause the speed of the dynamotor to oscillate above and below the required 60-cycle speed. With the anti-hunt circuit functioning, however, a current surge is sent through the feedback windings in a direction which aids the control windings to reduce the control-field current. The dynamotor will then increase its speed to correct for its initial drop in frequency caused by the line-voltage drop. Thus, the transient circuit and the feedback windings on the saturable reactor supplement the action of the sensing circuits and control windings.

THEORY AND METHODS OF DESIGN

Dynamotor and Field Winding

The design of the frequency-control system in this problem is concerned with one particular dynamotor unit, but the same principles are applicable to other machines of

similar character, both motor-generator sets and inverters. The dynamotor used in this system is a Janette type CA-19G Rotary Inverter (described in Appendix 1). A circuit diagram of the dynamotor in its original form is shown in Figure 5.

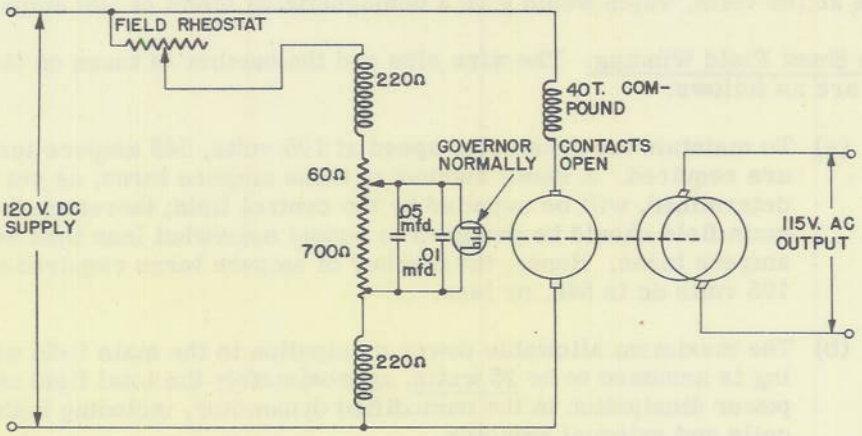

Figure 5 - Schematic diagram of original dynamotor unit

In order to derive the most satisfactory electrical efficiency from the dynamotor, it was necessary to rewind the field coils. A fixed shunt-field winding was used, along with an auxiliary field winding for control purposes. A small differential-compound motor-field winding was also added to the original windings as an additional means of obtaining speed stability. During the starting period, the compounding field is cut out by a small centrifugal switch on the dynamotor unit.

In this machine, a common field is used to excite both the d-c and the a-c windings. The field rheostat is a part of an electromechanical frequency-control system and is adjusted by a servo-mechanism to maintain the frequency at 60 cycles per second. The centrifugal governor contacts are normally open when the dynamotor is at a standstill. The governor is used for coarse speed control and as a speed limiter.

The over-all electrical efficiency of the original dynamotor was found to be low, (about 25 watts was dissipated in the field circuit alone), but little could be done to improve this condition. In order to keep the proposed magnetic amplifier small, it was necessary to divide the field windings into two separate sets of coils, namely, a fixed shunt field and a control field, the latter to be excited by the magnetic-amplifier output. The fixed shunt field, excited directly from the d-c supply, was designed as compactly as possible to make room for the control winding.

A series of performance tests on the original dynamotor was made and the results are shown in Appendix 1. For the extreme conditions of supply voltage and load range, the maximum and minimum field ampere turns were determined. In the proposed design, the minimum ampere turns for operation at 105 volts and full load must be supplied by the fixed shunt-field coils, and the additional ampere turns required for speed control must be supplied by the control-field coils. The shunt field was redesigned to operate without an external field resistance in order to avoid power waste. Excerpts from the original test data of the dynamotor (Appendix 1) show that a minimum shunt field of 448 ampere turns at 105 volts was required to maintain the speed of the machine under heavy load and low supply voltage. A preliminary investigation showed that the burden on the magnetic

amplifier could be reduced by the use of a differential compound field. To allow for the demagnetizing effect of a differential compounding field in the final design, the minimum value of 448 ampere turns was assumed to be 548 (based upon the estimated requirement of a differential compounding field of 40 turns and a maximum armature current of 2.5 amperes at 105 volts, which would give a demagnetizing effect of 100 ampere turns).

The Shunt Field Winding. The wire size and the number of turns on the shunt-field winding are as follows:

(a) To maintain the dynamotor speed at 105 volts, 548 ampere turns are required. A small number of these ampere turns, as yet undetermined, will be supplied by the control field; therefore the main field should be designed to supply somewhat less than 548 ampere turns. Hence, the number of ampere turns required at 105 volts dc is 548, or less.

(b) The maximum allowable power dissipation in the main field winding is assumed to be 25 watts, approximately the total field circuit power dissipation in the unmodified dynamotor, including both the coils and external resistor.

(c) At 125 volts dc, the required field resistance will be

$$R_f = \frac{125^2}{25} = 625 \text{ ohms.}$$

(d) At 105 volts, the field current will be

$$I_f = \frac{105}{625} = 0.1675 \text{ ampere.}$$

(e) To obtain 548 ampere turns at 105 volts dc, the number of turns required is

$$N = \frac{548}{.1675} = 3270 \text{ in two coils.}$$

(f) The resistance of the field winding will be

$$R_f = \frac{\rho l_c N}{A},$$

where

R_f = 625 ohms,

ρ = 10.4 ohms per mil foot,

N = 3270 turns,

l_c = 1.1 feet (length of mean turn),

and A = Cross-sectional area of conductor in circular mils.

(g) Solving for A:

$$A = \frac{10.4 \times 1.1 \times 3270}{625} = 60 \text{ CM.}$$

The nearest standard wire size for this cross-sectional area is No. 32 wire, with an area of 63.2 CM. However, as mentioned previously, the ampere turns should be 548 or less. No. 32 wire would give more than 548 ampere turns, while No. 33 wire, with an area of 50.1 CM, would give fewer than 548 ampere turns. No. 33 wire was therefore chosen as the best wire size for the design. Using 3270 turns of No. 33 wire, the resistance of the field will be increased to 746 ohms, and the power dissipation will be reduced to 21 watts.

(h) To bring the power dissipation back to the originally assumed value of 25 watts, it is necessary to bring the field resistance back to 625 ohms. Thus, for No. 33 wire:

$$625 = \frac{10.4 \times 1.1 \times N}{50.1}$$

or

$$N = 2730 \text{ turns.}$$

The ampere turns at 105 volts remains at 460 with No. 33 wire. This number of ampere turns will give a difference of 548 - 460 or 88 ampere turns to be supplied by the control field at 105 volts dc. This minimum value of 88 ampere turns as supplied by the control field is advantageous from the standpoint of magnetic-amplifier design because the magnetic amplifier does not need to reduce the control-field current to zero or even to a very low value. Thus the control-range requirements of the magnetic amplifier are lessened.

The actual winding is divided into two coils of 1350 turns each, with a resistance of 285 ohms per coil. The power dissipation in the two coils is 19.3 watts at 105 volts input, or a maximum of 27.4 watts at 125 volts. The temperature rise for this design was found not to be excessive under actual operating conditions.

The Control-Field Winding. The design of the control field for the dynamotor is closely associated with that of the magnetic amplifier. In general, it is desirable to design the fixed field of the dynamotor for compactness, and to allow as much of the remaining winding space on the field poles as possible for the control windings. The control-field coils should be designed to obtain the greatest number of ampere turns for the least power expended. In this way, the smallest and most efficient magnetic amplifier can be used, with a minimum of drain of control power from the a-c output side of the dynamotor.

From the dynamotor test data of Appendix 1, it is found that a maximum value of approximately 300 ampere turns of control field is necessary to maintain constant speed at no a-c load and maximum supply voltage. A minimum value of 88 ampere turns has already been determined. A conservatively designed magnetic amplifier will control over a somewhat wider range than that actually required.

The total available winding space for control winding on the two field poles of the dynamotor was found to be 0.75 square inches, allowing 0.11 square inches for the shunt field, and 0.06 square inches of estimated space required for a series field.

The required 300 ampere turns in the control winding can be obtained by a wide range of wire sizes and control currents. However, the control current must be supplied by the a-c output of the dynamotor itself, and there are voltage drops across the saturable reactors

and the field rectifier as well. It is desirable, therefore, to make the maximum d-c voltage across the control field considerably less than the a-c output voltage. Consequently, it is assumed that the 300 ampere turns can be obtained with a d-c impressed voltage of 75 volts.

Using the estimated impressed voltage, and knowing the available winding space and ampere-turn requirements, the wire size and the number of turns are found as follows:

(a) The total area of copper is the winding space times the space factor, or

$$A_c = 0.75 \times 0.4 = 0.3 \text{ sq. in. or } 381 \times 10^3 \text{ circular mils.}$$

The mean length of turn, l_c, was found to be 1.21 feet, allowing for the fact that the control-field coils are wound on top of the shunt-field coils.

(b) The number of turns of wire is found as follows:

$$N = \frac{E \times A_c}{\rho \, l_c (NI)}$$

or

$$N = \frac{75 \times 381 \times 10^3}{10.4 \times 1.21 \times 300} = 7550 \text{ turns.}$$

(c) The cross-sectional area of the copper is

$$\frac{381 \times 10^3}{7550} \text{ or } 50.5 \text{ CM.}$$

The nearest wire to this size is No. 33 wire, with an area of 50.1 CM.

The measured resistance of this winding, 1853 ohms, is capable of supplying 300 ampere turns with a control current of only 0.04 ampere. At a maximum impressed d-c voltage of 74 volts, the power dissipated in the shunt and control fields (at 125 volts input and no load) is therefore estimated to be as follows:

Shunt field of 548 ampere turns:	27.4 watts
Control field of 300 ampere turns:	2.9 watts
Total:	30.3 watts

Thus, for a limited amount of winding space, a pair of field coils is designed with five watts more power dissipation than that of the original dynamotor field but with the addition of a sensitive control field requiring less than three watts.

The Differential Compound Field Winding. In order further to minimize the control-range requirements of the magnetic amplifier or, in other words, to reduce the ratio of the maximum to minimum impedances of the saturable reactors, a differential compounding field is added to the dynamotor. It might be assumed that a differential compounding field

could be designed that would give perfect speed regulation under all conditions of load and supply voltage and that a magnetic amplifier and frequency-sensing circuit could be entirely eliminated. However, it is well-known that such an arrangement is not practicable because a nonlinear magnetic circuit, armature reaction, and other factors would make it impossible to obtain exactly the right amount of differential compounding under all conditions. It follows, therefore, that a practical approach to the problem is to use some differential compounding to relieve the magnetic amplifier of most of the burden of speed regulation and to obtain from the magnetic amplifier itself the few additional ampere turns required for fine speed regulation.

The following method was used in the design of the differential compound field winding:

(a) The dynamotor was tested, with the modified shunt-field windings and control-field windings in place, under extreme load and voltage conditions. The following results were obtained:

TABLE 1

D-C Line Volts	D-C Line Current (Amperes)	A-C Load	Power Factor	Frequency (cps)	Dynamotor Control Winding Current (Amperes)	Dynamotor Control Field Ampere Turns (For 7550 Turns)
108	2.1	80 watts	0.9	60	0.0005	3.78
122	1.4	0 watts	0	60	0.04	302.00

From Table 1, the ratio of maximum to minimum control ampere turns is found to be 80 to 1. It follows that the saturable reactors of the magnetic amplifier must change their impedance by a ratio greater than 80 to 1 in order to regulate current to the control-field rectifier which is in series with the reactors (Figure 2).

(b) Using the remaining winding space on the field poles of the dynamotor, a differential compound winding of 20 turns per pole of No. 18 wire, or a total of 40 turns, was added. This was not necessarily an optimum number of turns, but rather it was a compromise between available space and permissible IR drop through the series coils.

(c) More tests were made on the dynamotor with the series coils in place and under the same conditions as in (a) above. The ampere turns of the compounding field were then bucking the control winding ampere turns. This bucking effect was least when the armature current was small and the machine was running light, and greatest when the machine was drawing heavy armature current at full load. Thus, it was required to increase the magnitude of the control current in order to buck the compound field and to maintain constant speed.

TABLE 2

D-C Line Volts	D-C Line Current (Amperes)	Compound Field Ampere Turns (For 40 turns)	A-C Load Watts	Power Factor	Frequency (cps)	Control Winding Current (Amperes)	Control Winding Amp. Turns (For 7550 Turns)
122	1.4	56	0	0	60	0.0474	358
108	2.1	84	80	0.9	60	0.0116	87.78
110	---	--	100	--	60	0.0072	54.4

From Table 2, the new ratio of maximum to minimum control ampere turns is 358/87.78 = 4.08, as compared to the ratio of 80 in Table 1.

Thus the effect of the differential compound field has been to reduce by a factor of about 20 the ratio of maximum to minimum control ampere turns as well as the impedance range of the magnetic amplifier. The minimum current in the control field has also been raised from 0.5 milliampere to 11.6 milliamperes, and the a-c input to the control-field rectifier has increased in the same ratio. This is advantageous because it enables the saturable reactors to operate over a more effective part of their control range, the choice of a control range of 4 to 1 having proved to be close to the optimum value.

A schematic diagram of the modified dynamotor is shown in Figure 6. In order to start this machine at a low peak current value, it was found to be necessary to add some form of starting relay to the circuit. The use of a centrifugal switch from a small split-phase induction motor was found to be a satisfactory means of short-circuiting the compound field winding during the starting period.

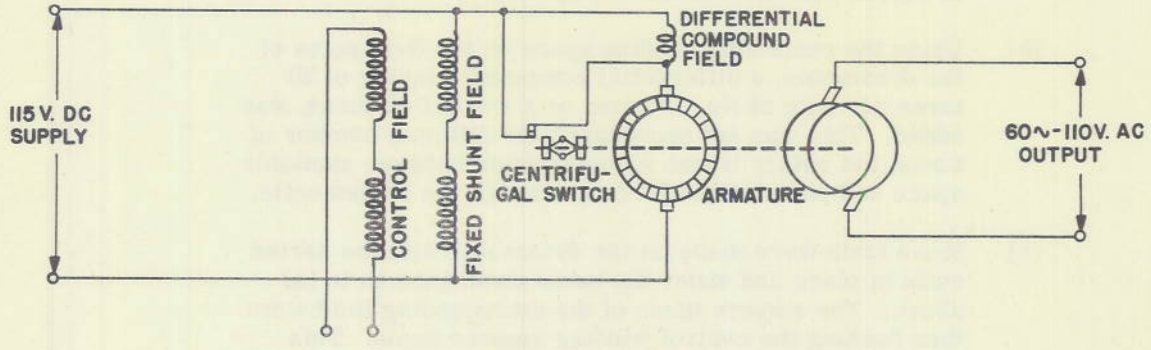

Figure 6 - Schematic diagram of modified dynamotor unit

Summary of Modified Field Winding Specifications. To summarize the modified field winding specifications for the Janette Type CA-19G Inverted Rotary Converter:

Shunt Field

Two coils, 1350 turns each, No. 33 Formex Insulated magnet wire.

Resistance: 285 ohms per coil.

Maximum power dissipation per coil: 13.7 watts at 62.5 volts per coil.

Control Field

Two coils, 3775 turns per coil, No. 33 Formex wire.

Resistance per coil: 926 ohms.

Power dissipation per coil (at 300 ampere turns): 1.45 watts (or a total power of 2.90 watts for the control field).

Differential Compounding Field

20 turns per pole, No. 18 Formex wire.

The Control-Field Rectifier. To supply direct current to the control field of the dynamotor, a full-wave dry-disc rectifier, shown in the circuit of Figure 2, was used. The data on the modified field windings of the machine show that the rectifier is required to supply a maximum of 47 milliamperes at 69 volts. A standard G. E. Copper Oxide Rectifier, Model 6RC3B125, was selected for the purpose. The following ratings apply to the rectifier:

Normal ac volts: 78

Normal dc volts: 58

Normal dc amperes: 0.11.

These ratings are slightly exceeded when the dynamotor runs at no load and 125 volts dc, but this extreme condition is not ordinarily encountered.

A 40-microfarad, 450-volt electrolytic filter condenser is connected across the rectifier output to smooth out ripple from the saturable reactor output of the magnetic amplifier.

The Frequency-Sensing Circuits

General Conditions. Before a magnetic amplifier can be designed to supply the required current to the auxiliary control field, a frequency-sensitive circuit is needed to control the amplifier. The design problems involving the range and sensitivity of the magnetic amplifier depend to a large extent upon the magnitude and rate of change of the d-c control currents that can be made available from the frequency-sensing circuits.

At the beginning of the investigation, it was assumed that the frequency-sensing circuit of Figure 2 would be the most suitable type to use; therefore the design that follows is based upon this original assumption.

The first reactors tried in this problem were used in a pair of tuned circuits operating in the vicinity of 60 cps. A Q value of about 72 was achieved in these reactors using laminated core construction of standard punchings of "4750" magnetic material. Insofar as the Q values were concerned, the reactors were satisfactory, but the performance of the sensing circuits when operated across the a-c output of the dynamotor was unsatisfactory.

The resonant circuits and their rectifiers formed a closed loop, and this loop, in turn, was shunted by the a-c windings of the dynamotor and the external load. Thus the a-c windings, as well as the load, appeared like phase-shifting networks to the tuned circuits. Any change in the ratio of reactance- to resistance-values in the generator or load would detune the resonant circuits to the extent that an excessively large error in frequency resulted. For these reasons, all attempts to operate the resonant circuits across the a-c windings of the generator were abandoned.

In order to overcome the detrimental effects of power factor and load change on the frequency characteristics of the two resonant circuits, it was decided to excite the frequency-sensing circuits from an independent alternator of small size driven from the shaft of the dynamotor. It is desirable to use a frequency higher than 60 cps to excite the resonant frequency-sensing circuits because of the resulting smaller values of inductance and capacitance. A power source of 240 cps was selected because of the availability of a small 8-pole, permanent-magnet alternator which was direct-connected to the shaft of the dynamotor. A higher frequency would have been desirable from the standpoint of high-Q reactor design. It was found, however, that the efficiency of available types of dry-disc rectifiers dropped off at the higher frequencies to the extent that the over-all Q of the tuned circuits, including the rectifiers, was lower even though the Q of the reactors was better at the higher frequencies.

The design of the frequency-sensitive circuits takes into account factors other than the Q of the reactors. Among these considerations are:

(a) Maintenance of frequency control to 0.1 percent over a temperature range of 40° to 130°F;

(b) The available a-c voltage for exciting the resonant circuits (240-cycle generator);

(c) The peak voltages and currents across the reactors and condensers of the circuit at resonance;

(d) The a-c voltage limitations of the rectifiers;

(e) The I^2R losses in the reactor and voltage source;

(f) Transient voltages across the reactors.

Temperature-Stabilized Toroid Reactors. The most successful design of tuned circuit reactors was the toroid-coil type shown in Figure 7. It was found that the problem of temperature stability over the required operating range of the frequency-control system outweighed all of the other problems of design. For this reason it was found to be advisable to compromise on the high Q requirements of the sensing reactors, provided that an adequate amount of control current could still be obtained from the two tuned circuits near resonance.

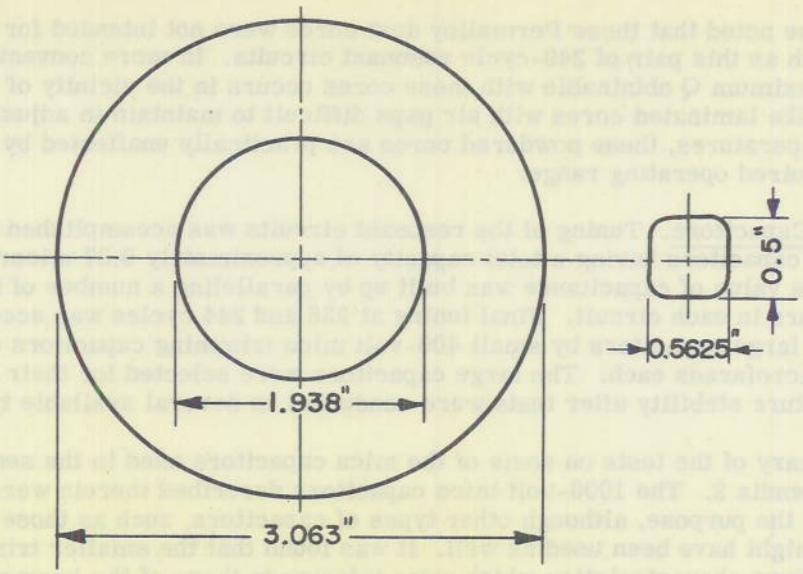

Western Electric Permalloy-Dust Cores
μ 125, KES-637627-1, BTL ESP-637627
2.1 cu. in. Wt 0.058 lb
#3 finish
Winding Specifications:
3500 turns 28 wire
2890 turns 26 wire in series on each core
Inductance: 6 Henrys

Figure 7 - Outline drawing and winding specifications for powdered metal core reactors

It was found that a commercial type of temperature-stabilized core was adequate to meet the performance requirements of the frequency-sensing circuits in this problem. This core is in toroid form and is molded from Permalloy dust in a standard size having the following specifications:

Type: Western Electric No. KES-637627-1 (μ125 Core)

Temperature stability: ±0.1% (in permeability) from 30°to 130°F.

Dimensions: Outside diameter = 3.06 inches.

Inside diameter = 1.94 inches.

Thickness = 0.5 inch.

Volume = 2.1 cubic inches.

Weight = 0.58 pound.

By the use of this available type of toroid core, it was found practicable to obtain an inductance of approximately 6 henrys with a coil of 6390 turns. The Q of the coils was approximately 25.

It is to be noted that these Permalloy dust cores were not intended for use in an application such as this pair of 240-cycle resonant circuits. In more conventional applications, the maximum Q obtainable with these cores occurs in the vicinity of 5000 cycles per second. Unlike laminated cores with air gaps difficult to maintain in adjustment over a range of temperatures, these powdered cores are practically unaffected by temperature over the required operating range.

Tuning Capacitors. Tuning of the resonant circuits was accomplished by means of high-quality capacitors having a total capacity of approximately 0.07 micorfarads in each circuit. This value of capacitance was built up by paralleling a number of 0.01- and 0.25-mfd capacitors in each circuit. Final tuning at 238 and 244 cycles was accomplished by shunting the large capacitors by small 400-volt mica trimming capacitors of approximately 250 micromicrofarads each. The large capacitors were selected for their low power factor and temperature stability after tests were conducted on several available types.

A summary of the tests on some of the mica capacitors used in the sensing circuit is given in Appendix 2. The 1000-volt mica capacitors described therein were found to be adequate for the purpose, although other types of capacitors, such as those having a plastic dielectric, might have been used as well. It was found that the smaller trimmer condensers had temperature characteristics which were inferior to those of the larger, high-voltage condensers; however, the trimmers contribute only a small percentage of the total capacitance required, and they likewise contribute very little to the temperature drift of the tuned circuits.

Rectifiers. Standard commercial rectifiers of the selenium full-wave bridge type were found suitable as rectifiers to be inserted in series with the two resonant circuits. In selecting rectifiers for this application, it is important to consider their temperature stability, current, and peak a-c voltage rating. For temperature stability in the vicinity of 130°F, the selenium rectifier was found to be superior to its equivalent in the copper-oxide type. The rectifiers must have a low impedance in order to keep the Q of the resonant circuits at a high value for frequency sensitivity. At the same time, the pilot-generator voltage must be kept as low as possible to limit the peak voltages across the circuit components at resonance. Any series impedance contributed by the rectifiers makes it necessary to raise the generator voltage to higher levels for a given sensitivity.

The following specifications apply to the rectifiers found to be satisfactory in this application:

Type: Single-phase full-wave circuit - 1 inch diameter cells.

Manufacture: General Electric, Model 6RS42F1.

Maximum Rating: 24 volts, 0.25 ampere dc.

31 volts ac.

Pilot Generator. The auxiliary or pilot alternator was a small eight-pole, three-phase generator having the following electrical characteristics:

Frequency: 240 cps

Poles: 8

Phase: 3

Connection: Delta

Voltage: 15

Approx. current/phase: .040 ampere

Slots/pole/phase: 2

As shown in Figure 2, the frequency-sensing circuits were connected to separate phase windings of the pilot generator. This arrangement was used because it reduced interaction between the two tuned circuits. The wave form of the pilot generator was nearly sinusoidal.

Performance Data. The performance curves, as well as the circuit constants for the resonant circuits, are shown in Figure 8. It is to be noted that, in the actual performance data shown in Figure 8a, the cross-over point of the resonance curves is purposely set at 60.1 cycles per second instead of at 60. At exactly 60 cycles there is a difference of 3 ampere turns required to buck out a slightly excessive amount of biasing ampere turns caused by the self-excitation circuit (to be described later). This method of correcting for too much self-excitation can be justified only when the required correction is small, as in this case. Since the frequency-sensing circuits are independent of load or voltage changes in the power circuits of the dynamotor, it is practicable to operate the resonant circuits slightly away from the cross-over point without sacrifice of accuracy or stability.

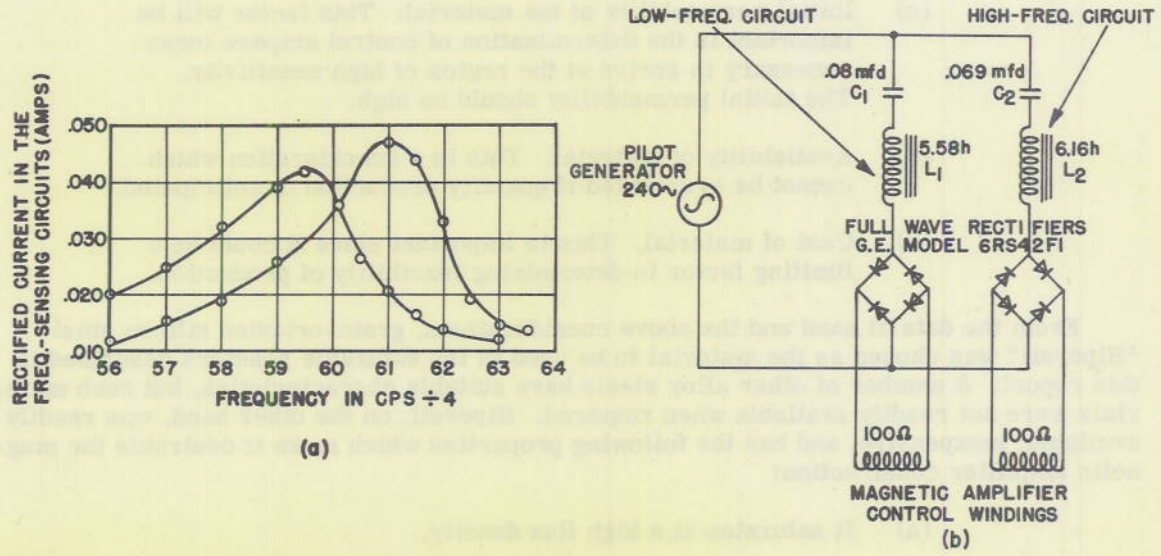

Figure 8 - Resonance curves and constants of the frequency-sensing circuits

The Magnetic Amplifier

There are a number of ways to approach the problem of designing saturable core reactors for a specific purpose. These methods are discussed at length in the literature, but in general the methods are either of an empirical nature or in the form of mathematical analyses. The methods given here are both analytical and empirical, and have proved to be effective for the type of amplifier concerned.

Selection of Core Material. The first design consideration is the selection of the reactor cores. Since the magnetic materials as furnished by manufacturers at the present time do not conform very closely to their published specifications, it is not practicable to use the manufacturers' saturation curves for design purposes. Instead, it is necessary to make individual saturation tests on the material to be used. This procedure, of course, necessitates the procurement of sample cores before the actual core size is known. However, a first approximation to the correct core size can usually be determined from the manufacturers' published data.

Some important factors to be considered in choosing the type of magnetic material to be used are the following:

(a) Incremental permeability of the material. The highest incremental permeability is desirable because excitation currents are inversely proportional to permeability and it is advantageous to keep excitation currents low, as will be shown later.

(b) The flux-density value at the knee of the saturation curve. The knee of the saturation curve should be at as high a flux-density value as possible, since this location eventually will result in a saving in core material and copper for the windings.

(c) Initial permeability of the material. This factor will be important in the determination of control ampere turns necessary to arrive at the region of high sensitivity. The initial permeability should be high.

(d) Availability of material. This is a consideration which cannot be overlooked if quantity production is anticipated.

(e) Cost of material. This is important since it could be a limiting factor in determining feasibility of production.

From the data at hand and the above considerations, grain-oriented silicon steel "Hipersil" was chosen as the material to be used in the saturable reactors described in this report. A number of other alloy steels have suitable characteristics, but such materials were not readily available when required. Hipersil, on the other hand, was readily available, inexpensive, and has the following properties which make it desirable for magnetic amplifier construction:

(a) It saturates at a high flux density.

(b) The permeability is high, even at high flux-density values.

(c) The power transfer per unit volume of core is better than that of most nickel-alloy materials.

(d) Hipersil contains no nickel or other critical materials.

(e) Hipersil can be obtained in ribbon form for winding into toroid cores, the most effective type of core configuration for low magnetic and copper losses.

Core Shape. Since these cores are to be used as saturable reactors, and since it is desirable to saturate the cores with a minimum of power applied to the d-c control windings, it follows that the best design will be one having the greatest possible window space for the winding without too long a reluctance path. These requirements indicate a core configuration where, in a closed loop of magnetic material, the area of the enclosed loop is maximum with respect to the perimeter. This condition is satisfied by circular toroid.

To illustrate the advantages of the circular core shape, consider the cores shown in Figure 9. In Figure 9a the square window opening of the core has an inside perimeter of 4L, and the area of window opening is $A = L^2$. This core is compared with Figure 9b which has an inside circumference equal to 4L (or an inside diameter of $4L/\pi$). The area of window opening for the toroid is

$$A' = \frac{\pi D^2}{4} = \frac{\pi(4L)^2}{4(\pi)} = \frac{4L^2}{\pi} = 1.273L^2 .$$

Thus, the ratio of window areas for the toroidal and the square cores is

$$\frac{A'}{A} = \frac{4L^2}{\pi} \div L^2 = \frac{4}{\pi} = 1.273.$$

Since the mean lengths of the magnetic paths in Figures 9a and 9b are approximately in direct proportion to L, it can be said that, for the same length of path, the toroid core has a 27.3% advantage over the square core in available window area or winding space. To show further the advantage of the toroid core from the standpoint of facility of winding the coils, it can be demonstrated that the 27.3% excess window area of the toroid is equivalent to a hole having a diameter of 0.58L. This means that if the square window opening in Figure 9a were completely filled with wire, the same number of turns wound on the toroid would still leave at the center an opening of diameter 0.58L. It can also be shown that the mean length of turn for the toroid core is less than that of the square cross section because of the opening that remains in the toroid center. The copper loss of the toroid will therefore be less than that of the square core.

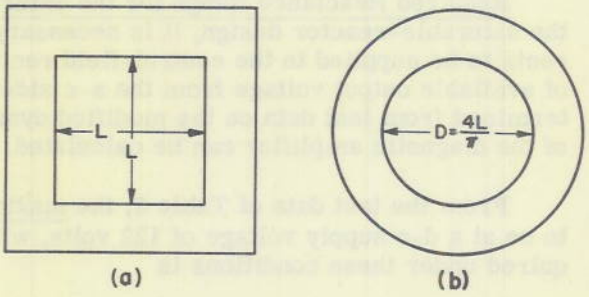

Figure 9 - Two core configurations

To summarize, the advantages of the toroid core construction are:

(a) More winding area (window area) is available for a given length of magnetic path, or conversely, the minimum reluctance path for a given number of turns of wire is obtained.

(b) The copper loss of the toroid winding is less because the mean length of turn is less than that for other core shapes.

(c) The toroid construction makes possible the use of ribbon core material having superior magnetic properties of its own, and with practically no air gaps across the main flux path.

(d) Commercial practice indicates that toroidal cores can be wound in production to a final hole diameter of 1/4 inch. Thus, for cores with an inner hole of 1/2-inch diameter or larger, the toroidal core is the most advantageous one to use.

The advantages of toroid-coil construction are well known in the communication field, and the above analysis is given only because the square window core is sometimes used by magnetic-amplifier designers where the toroid core would give superior performance.

Some experimental reactors were made from standard punched laminations of the type used in ordinary transformer construction. Laminations such as the EI type were easy to assemble, and they produced quite satisfactory reactors when interleaved stacking was used. A number of reactors of such conventional construction were made from Mu-Metal and 4750 nickel alloy early in this problem. However, these reactors were found to have the serious disadvantage of lack of uniformity of the air gaps, even with interleaved construction. Two apparently identical reactors would show widely different magnetic saturation values, and it was almost impossible to select a pair with characteristics close enough together to make them operate in a common circuit. Mainly because of this disadvantage, the conventional EI core construction was abandoned.

Required Reactance Range for the Saturable Cores. In order to proceed further with the saturable-reactor design, it is necessary to know the range of a-c voltages and currents to be supplied to the control-field rectifier. It is also necessary to know the range of available output voltage from the a-c side of the dynamotor. When these values are determined from test data on the modified dynamotor, the maximum and minimum reactances of the magnetic amplifier can be calculated.

From the test data of Table 2, the maximum current to the control winding is found to be at a d-c supply voltage of 122 volts, with no load on the dynamotor. The current required under these conditions is

$$I_{c_{max}} = 47.4 \text{ ma (direct current).}$$

The maximum a-c input to the rectifier is, therefore,

$$I_{ac} = 1.11 \times 47.4 = \underline{52.6 \text{ milliamperes}} \text{ (rms)}$$

for a full-wave rectifier. From Table 2, the minimum current to the control winding is

$$I_{c_{min}} = 11.6 \text{ ma,}$$

and the minimum ac is

$$I'_{ac} = 1.11 \times 11.6 = \underline{12.9 \text{ milliamperes}}$$

for a full-wave rectifier.

Since the control field has a measured resistance of 1853 ohms, the maximum a-c voltage impressed upon the control field rectifier is

$$E_{ac_{max}} = 1853 \times .0526 = 97.5 \text{ volts},$$

and the minimum a-c voltage is

$$E_{ac_{min}} = 1853 \times .029 = 23.9 \text{ volts}.$$

At no load and at maximum supply voltage, the a-c voltage of the dynamotor rises to 133 volts. The voltage drop through the reactors under these conditions is, therefore,

$$E_x = \sqrt{133^2 - 97.5^2} = 90.4 \text{ volts (rms)}.$$

At a supply voltage of 108 volts and an a-c resistive load of 80 watts, the dynamotor a-c voltage is 99 volts. Under these conditions, the reactor voltage drop required is

$$E'_x = \sqrt{99^2 - 23.9^2} = 96.0 \text{ volts (rms)}.$$

From the above voltages and currents, the effective inductance of the current-controlling reactors must vary between 20 and 4.6 henrys.

For an idealized magnetic amplifier of this arrangement, it may be shown that the equivalent inductance of the combined a-c windings is one-half of the inductance of one a-c winding alone. Therefore, the upper and lower values of operating inductance of one a-c winding should be 40 and 9.2 henrys respectively.

These values are the inductances required to maintain a frequency of 60 cps through the rated load range. This, however, leaves no margin of control for an overload. Thus, in anticipation of overload, the inductance range must be increased. In this design an overload condition of 100 watts with input voltage to the dynamotor held at 110 volts dc was taken as the limit. With this overload the direct current to the control field is 0.0072 ampere. The equivalent alternating current through the reactor at this condition is

$$I'_{ac} = 1.11 \times 0.0072 = 0.008 \text{ ampere (rms)}$$

and the a-c voltage is

$$E_{ac} = 1853 \times .008 = 14.824 \text{ volts (rms)}.$$

The a-c voltage output from the dynamotor is 93 volts. With these conditions the reactor voltage drop is

$$E_x = \sqrt{93^2 - 14.824^2} = 92 \text{ volts}.$$

The effective inductance at this condition is 30.6 henrys. Thus, the upper limit of operating inductance will be 61.5 henrys.

Determination of Core Volume and Dimensions. The volume of core material required for a saturable reactor can be found from the mathematical relationship that exists between the volume, the flux density, and the inductance values. From the formulas for inductance and flux density:

$$L = \frac{N\phi}{I} \times 10^{-8} \text{ henrys,} \tag{1}$$

where N is number of turns on the reactor coil, I is the effective current through the reactor, ϕ is the effective flux in the reactor core, and L is the inductance in henrys.

Now,

$$\phi = \frac{0.4\,\pi N I \mu A}{l_m}, \tag{2}$$

where A is the cross-sectional area of the core and l_m is the effective length of the magnetic path in centimeters. Substituting (2) in (1),

$$L = \frac{.4\pi N^2 A\,\mu \times 10^8}{l_m} \text{ henrys.} \tag{3}$$

The peak value of flux density, B_m for a sine-wave voltage is:

$$B_{max} = \frac{\sqrt{2} \times 0.4\pi N I \mu}{l_m}. \tag{4}$$

Solving for N in equation (4),

$$N = \frac{B_m \times l_m}{\sqrt{2} \times .4\pi\,\mu I}. \tag{5}$$

Substituting (5) into (3), the equation becomes

$$L = \frac{K_2\, B_m^{\,2} \left(l_m A\right)}{I^2 \mu}, \tag{6}$$

where

$$K_2 = \frac{1}{0.8\,\pi \times 10^8}.$$

Since the volume of the core = $l_m A$ (approximately),

$$V_i = \text{volume of core} = \frac{L I^2 \mu}{K_2 B_m^{\,2}}. \tag{7}$$

It is to be noted that for any point on the saturation curve there is but one value for B_m and for μ. It follows that for a given value of current the volume of core material is a function of the inductance, the permeability, μ, and the flux density squared, $B_m^{\,2}$.

At any given point on the saturation curve, the voltage drop is proportional to $(l_m A)/I$, which indicates that the voltage drop is directly proportional to the volume of core material and inversely proportional to the current. Equation (7) also shows that the greater the value of B_m the smaller will be the required volume of core material.

However, it is to be remembered that the value of μ must be kept high in saturable reactors. The minimum current in the reactors should be kept low in order to maintain high operating effectiveness (i.e., the power consumed at maximum inductance, with no dc applied to reactor, should be negligible). The value of B_m should be located just below, but as near as possible to, the knee of the a-c saturation curve of the core material. The exact location of this point is somewhat arbitrary and in most materials is located above the values of B and H at which maximum a-c permeability occurs. The closer to the knee of the curve, this point can be located, the fewer the turns that will be required in the a-c winding for a given voltage drop. The value of minimum current is increased by moving the value of B_m toward the knee of the curve and is decreased by moving B_m downward on the curve and away from the knee. As the value of B_m is moved downward, however, the number of turns required for a given reactance drop will increase and will consume additional winding space. If a larger core cross-section were used, it would be possible to choose a point closer to the maximum permeability part of the saturation curve and still have a lower number of turns, but the mean length of turn with increased copper losses would tend to counteract the advantage gained by operating the core at a higher permeability. Thus, the choice of the maximum inductance point must be a compromise between maximum voltage drop required, minimum acceptable reactor current, available winding space, and copper loss.

Using the manufacturer's data on the magnetic material chosen for this application, the approximate volume of the core is found as follows: A value of B_m is chosen at 15,000 gauss. (The point is in the knee of the saturation curve, and the permeability, μ, is still high. This value is in accordance with requirements mentioned elsewhere in this section.) The value of μ at this point is 18,600. The inductance, L, is to be 60 henrys. The current is assumed to be 0.004 ampere. Thus, using equation (7)

$$V_i = l_m A = \frac{LI^2\mu}{K_2 B_m^2} = \frac{60 \times 16 \times 10^{-6} \times 18.6 \times 10^3}{3.98 \times 10^{-9} \times 225 \times 10^6}$$

$$= 19.8 \text{ cubic centimeters, or the volume of core required.}$$

Experimental Determination of Core Volume and Magnetic Characteristics. These calculations were checked experimentally on sample cores having approximately the calculated volume. The volume of each core actually selected was 19.2 cubic centimeters. The difference between the actual and calculated volumes was necessitated by size limitations of standard cores.

A diagram of the actual cores used and an experimental test circuit for obtaining a-c magnetization curves, are shown in Figure 10. An arbitrary test coil of 180 turns of No. 18 wire was wound on each core for the test. The data obtained on the two core samples are given in Table 3 and are shown graphically in Figure 11.

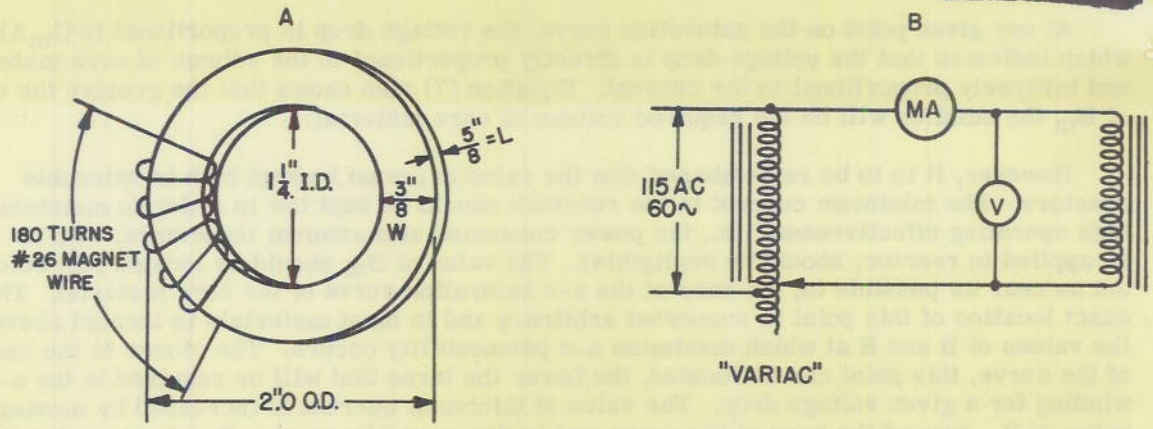

MATERIAL: WESTINGHOUSE HYPERSIL, 29 GAUGE
AREA OF CROSS SEC. = 0.233 in^2 = 1.5 cm^2
MEAN LG. OF MAGNETIC PATH = 5.1 in = 12.95 cm
VOLUME OF CORE = 1.17 in = 19.2 cm^3

Figure 10 - Diagrams of saturable reactor and test circuit

TABLE 3

A-C Volts	Core 1 A-C Milli-amperes	Core 2 A-C Milli-amperes	Core 1		Core 2	
			B_{max}	H_{max}	B_{max}	H_{max}
1	3.2	3.8	1402	0.079	1402	0.094
2	5.6	6.0	2804	0.138	2804	0.148
3	7.4	7.7	4210	0.183	4210	0.190
4	9.2	9.4	5610	0.226	5610	0.231
5	10.8	10.8	7020	0.266	7020	0.266
6	12.5	12.5	8420	0.308	8420	0.308
7	14.8	14.8	9830	0.364	9830	0.364
8	17.4	17.4	11220	0.428	11220	0.428
9	20.5	21.5	12620	0.504	12620	0.529
10	25.0	26.5	14020	0.615	14020	0.652
11	30.0	32.5	15420	0.740	15420	0.800
12	37.0	40.0	16850	0.913	16850	0.986
13	48.0	52.0	18250	1.182	18250	1.282

From the data of Table 3 and the curves of Figure 11, a point x (Figure 11) was located at approximately 15,000 gauss. This value corresponds to the previously chosen value taken from the manufacturer's data. At this point the actual permeability, μ, is about 20,000, slightly higher than the value of 18,600 given by the manufacturer. These two values of permeability are so close together that the core volume need not be changed.

Point x on the curve of Figure 11 is chosen to be the point corresponding to the flux density and magnetizing force which will exist in the cores of the saturable reactors when they are operating at the high limit of the inductance range for this application. This is the only point of operation which can be located on these curves because at any other point of operation the cores will have a d-c component of flux as well as the alternating flux. The curves of Figure 11 show alternating flux only.

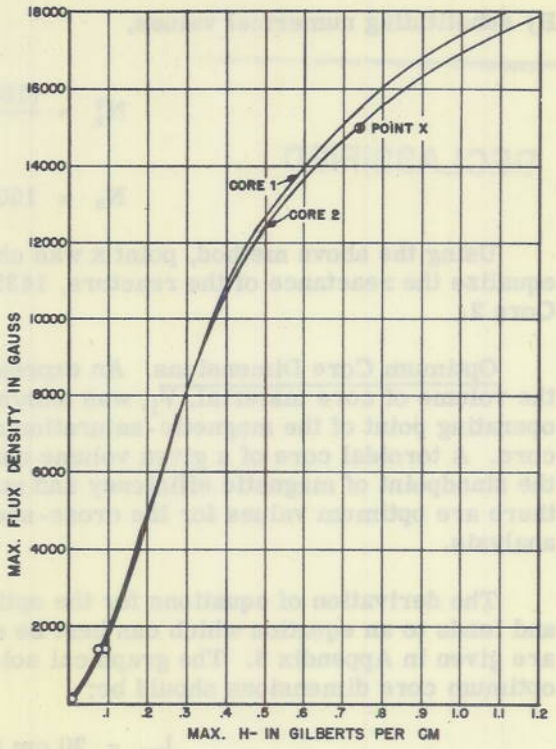

Figure 11 - Ac magnetization curve for two saturable reactor cores

The number of turns required to obtain an inductance of 61.5 henrys can now be determined. From Table 3 the voltage with the 180-turn coil is approximately 11 volts with a current of 0.0325 ampere. Thus the ampere turns at point x are approximately 6.0. The inductance of the test coil at point x is:

$$\frac{E}{I\omega} = \frac{11}{.0325 \times 377} = .896 \text{ henrys.}$$

The number of turns may be obtained by the following equations:

$$\frac{L_1}{L_2} = \frac{N_2^2}{N_2}$$

$$N_2^2 = \frac{N_1^2 L_2}{L_1}$$

where:

L_1 is the test coil inductance,

L_2 is the required inductance,

N_1 is the number of turns in the test coil, and

N_2 is the number of turns in the required reactor.

By substituting numerical values,

$$N_2^2 = \frac{(180)^2 \times 61.5}{.896} = 2{,}225{,}000, \text{ and}$$

$$N_2 = 1500 \text{ turns, approximately.}$$

Using the above method, point x was chosen on the curve for Core 2. In order to equalize the reactance of the reactors, 1435 turns were used on Core 1 and 1500 turns on Core 2.

Optimum Core Dimensions. An expression for the core volume has been derived, and the volume of core material, V_i, was shown to be dependent upon the minimum current operating point of the magnetic-saturation curve, i.e., where no d-c flux is present in the core. A toroidal core of a given volume can have a wide variation of dimensions, but from the standpoint of magnetic efficiency and minimum copper loss (or minimum control power) there are optimum values for the cross-sectional dimensions which require a more thorough analysis.

The derivation of equations for the optimum dimensions of the core is quite complicated and leads to an equation which can best be solved graphically. This derivation and solution are given in Appendix 3. The graphical solution shows that for a volume of 19.22 cc, the optimum core dimensions should be:

l_m = 20 cm (mean length of magnetic path);

W = 0.7 cm (radical thickness of core);

b = 1.4 cm (axial length of core).

In order to use available cores, it is sometimes necessary to deviate from these optimum relations. In such cases, it should be remembered that it is better to have a larger difference between the inner and outer diameters of the core rather than a smaller one. To minimize the effect of magnetic-potential gradient in a toroidal-shaped core, the ratio between the inner and outer diameters should be small. This effect, however, is less pronounced than the effect of NI/l_m (Appendix 3).

The core dimensions of Figure 10 were checked by the method given in Appendix 3. The dimensions of these cores were found not to be optimum values. However, the use of optimum values for cores of this volume (19.22 cc) would increase the effectiveness of the control winding by approximately 10 percent over the cores of Figure 10. Since the latter cores were available, they were used for the final model of the magnetic amplifier. As shown in Appendix 3, effectiveness of control winding is defined as the field strength per watt of control power.

The Self-Saturation Circuit. In order to utilize the core material mentioned in Figure 10 to better advantage, a "self-saturation" or "self-excitation" circuit can be applied. Although this type of circuit obviously cannot change the physical properties of a magnetic material to make it any better than it was after original manufacture and heat treatment, use of this circuit will result in a virtual magnetization curve having a sharper bend at the knee and a steeper initial slope. The self-saturation method has a cumulative effect which gives the reactors the performance characteristics that otherwise could be achieved only by the use of materials having a more sharply defined knee in their saturation curves.

A self-saturation circuit is shown in Figure 12. This circuit is frequently used in magnetic-amplifier designs to compensate in part for materials that do not have an ideally shaped magnetization curve for this application but do have other good properties that make them desirable in magnetic amplifiers. Grain-oriented silicon steel is an example of such a material. An important factor in connection with the self-saturation circuit is the choice of half-wave rectifiers capable of carrying the maximum ac in each reactor circuit. These rectifiers should have unusually low forward resistance and high back resistance at low values of current.

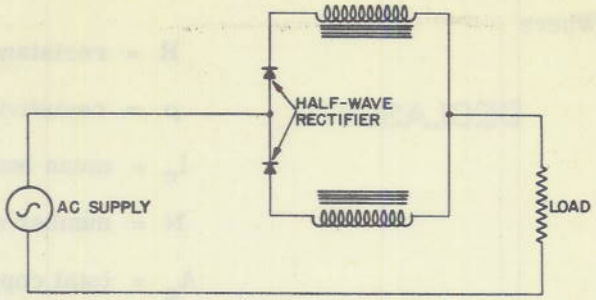

Figure 12 - A simple self-saturated circuit

The biasing ampere turns due to self-saturation vary with the load current through the reactors. In the case of the amplifier used in this development, the ampere turns of bias were not exactly the required value. In order to compensate for the ampere turns caused by this deviation from the required bias, the resonant circuits were tuned so that their currents were equal at a frequency slightly higher than 240 cycles per second. In this way, a difference in current is established between the two control circuits which yields just enough ampere turns to give the required bias value on the saturable reactors when the dynamotor is operating at exactly 60 cps. The ampere turns supplied for compensation by the frequency-sensing circuits must be small in order to be practicable.

Control Windings for Saturable Reactors. In order to get as much control sensitivity as possible from the resonant circuit signals, the control windings on the saturable reactors were designed to fill as much as practicable of the remaining winding space (in these reactors, this remaining space is 0.9 square inch).

It may be noted here that the sensitivity of the resonant circuits is inversely proportional to the resistance in these circuits. This relationship is true because, in a series circuit, the Q is inversely proportional to the resistance. For a high-Q circuit, therefore, the resistance of the control windings should be made low. In addition, the voltage across the L and C components in the resonant circuits must be kept down to a safe value. The latter requirement, of course, limits the current value through the resonant circuit components. It was found to be desirable to keep the resonant voltage across the L and C components below 400 volts; therefore, the maximum dc from the rectifiers is limited to approximately 40 milliamperes. At this current value, a-c potentials across the components are approximately 400 volts.

Considering the above factors, and the available generated emf of 15 volts from the pilot generator, the control winding resistance was found as follows:

A test run was made with various load-resistance values on the rectifiers. In this test, it was found that a 200-ohm load resistance yielded a rectified output current of 40 milliamperes. Thus, the value of 200 ohms was selected as the proper value for the control winding resistance.

The wire size was then determined by taking the available area for the control winding, the mean length of turn of copper, and the above resistance value, and solving for number of turns in the formula

$$R = \frac{\rho l_c N^2}{A_c},$$

where

R = resistance of winding

ρ = resistivity of copper wire

l_c = mean length of turn

N = number of turns

A_c = total copper cross-sectional area.

Solving for the number of turns,

$$N = \frac{RA_c}{l_c}.$$

In this case: $R = 200$, $l_c = 4.25$ inches, $A_c = 0.3$ square inch (allowing for 0.9 square inch of available winding area and a winding space factor of 0.33 for hard-wound coils), and $\rho = 0.885 \times 10^{-6}$ ohms per inch/3. Substituting these values in the above formula gives a value for N of 4000 turns. The wire size is then found by taking the total copper cross section, A_c, and dividing by number of turns, N. Thus, the cross-sectional area of wire = $A_c/N = 0.3/4000 = 0.000075$ square inch. This area corresponds to No. 30 wire as the nearest size. In the above design, the 4000 turns are placed on the toroids in four coils of approximately 1000 turns each.

Tests on the resonant circuits indicated that they were capable of providing more than adequate power for the control windings. At the same time, it was found that the anti-hunt windings were deficient by approximately 2000 turns, as required for stable operation. This deficiency in anti-hunt winding turns resulted from winding No. 37 wire by hand and from inaccurately estimating the space required for the anti-hunt windings. If smaller wire could have been used, the number of turns in the anti-hunt winding would not have been deficient and the design would have resulted in a control system somewhat better than the one actually developed. However, the deficiency of approximately 2000 turns per reactor of the anti-hunt winding was made up by removing this number of turns from the control winding and adding them to the anti-hunt winding. This, of course, somewhat reduced the effectiveness of the control circuits. However, the reduction in effectiveness was not enough to reduce the frequency-control sensitivity below the minimum requirements of the problem. Figure 13 is a curve showing the operating characteristics of the magnetic amplifier employing self-excitation. Points A and B on this figure show the limits of operation.

The Transient Feedback or Anti-Hunt Circuit. In a servo-mechanism such as the frequency-control system described herein, it is desirable to obtain the highest possible control sensitivity without loss of system stability. In systems of this kind, the required stability can be achieved electrically by a positive feedback circuit which operates only during the transient.

The feedback circuit used in this design is a series R-C & L circuit energized by the magnetic amplifier. This circuit feeds energy back into the amplifier through auxiliary windings on the saturable core reactors. The method of operation of this circuit with load and supply-voltage disturbances has already been described.

Analytical treatments of the servo-mechanism loop are to be found in the literature. However, it was found that empirical methods provided the quickest solution of this problem.

The first step in designing this anti-hunt circuit was to determine the hunting frequency of the control system when operated without a damping circuit. The frequency-control system was operated over the full required range of load and supply voltages. Meters inserted in the circuit at various points were used to detect oscillations. In this system, the hunting frequency was found to be about 1.5 cycles per second. This low frequency could readily be timed. If no hunting is observed in this method, the system either requires no anti-hunt circuit at all, or else it is operating below its optimum sensitivity.

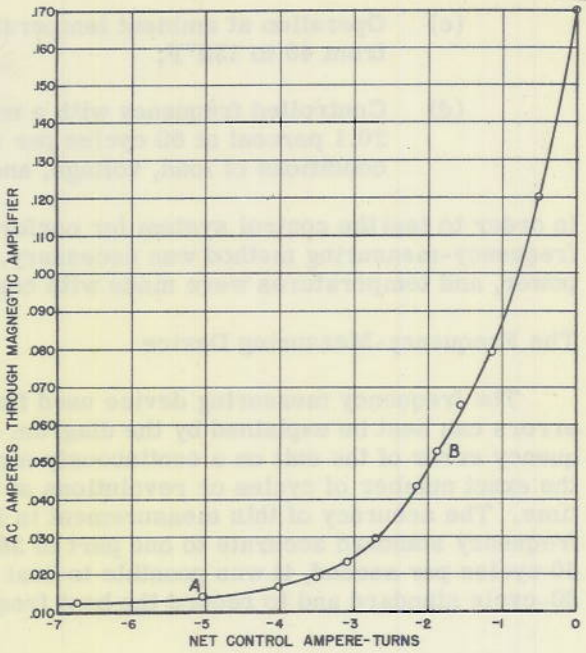

Figure 13 - Control Characteristic of magnetic amplifier used in frequency control system

The method used here to eliminate hunting increases the transient or frequency error rate sensitivity without affecting the steady-state sensitivity of the system. This is true because the anti-hunt circuit operates to aid the sensing circuit in restoring the frequency to its normal value, and the condenser in the normally d-c circuit causes it to function only during a change in frequency.

In the saturable reactors, the damping windings on each reactor consists of 3400 turns of No. 37 wire, plus 1000 turns of No. 30 wire per reactor (initially used in the control winding), in series with an electrolytic condenser of 180 microfarads. The total damping circuit has a resistance value such that the time constant of the resistance-capacitance combination is shorter than the period of hunt frequency.

The anti-hunt circuit is connected across the control-field rectifier. In general, a system of this sort is most effective when energized from the section of the control system which is operating at the highest power level.

EVALUATION OF THE FREQUENCY CONTROL

Evaluation of the constant-frequency control system was made after completion of design and construction of the model. Tests already reported on the various components were made during design of the system to serve as a guide for necessary changes in construction. The results reported here are final evaluation tests on the individual parts as well as on the system as a whole.

As stated earlier in the report, the requirements for the system are:

(a) Operation under load conditions ranging from zero to full load;

(b) Operation with supply-voltage variations ranging from 109.25 to 120.75 volts;

(c) Operation at ambient temperatures ranging from 40 to 130°F;

(d) Controlled frequency with a maximum error of ±0.1 percent at 60 cycles per second under all conditions of load, voltage, and temperature.

In order to test the control system for conformance to these requirements, an accurate frequency-measuring method was necessary. The measurements of voltages, currents, power, and temperatures were made with conventional instruments.

The Frequency-Measuring Device

The frequency measuring device used for checking actual frequency and deviation errors can best be explained by the diagram of Figure 14. This device records the frequency error of the unit on a continuously moving chart so that it is possible to determine the exact number of cycles or revolutions of the dynamotor lost or gained in a unit of time. The accuracy of this measurement is limited only by that of a crystal-controlled frequency standard accurate to one part in 26,000. Thus with a standard frequency of 60 cycles per second, it was possible to beat the dynamotor output frequency against the 60-cycle standard and to record the beat frequency.

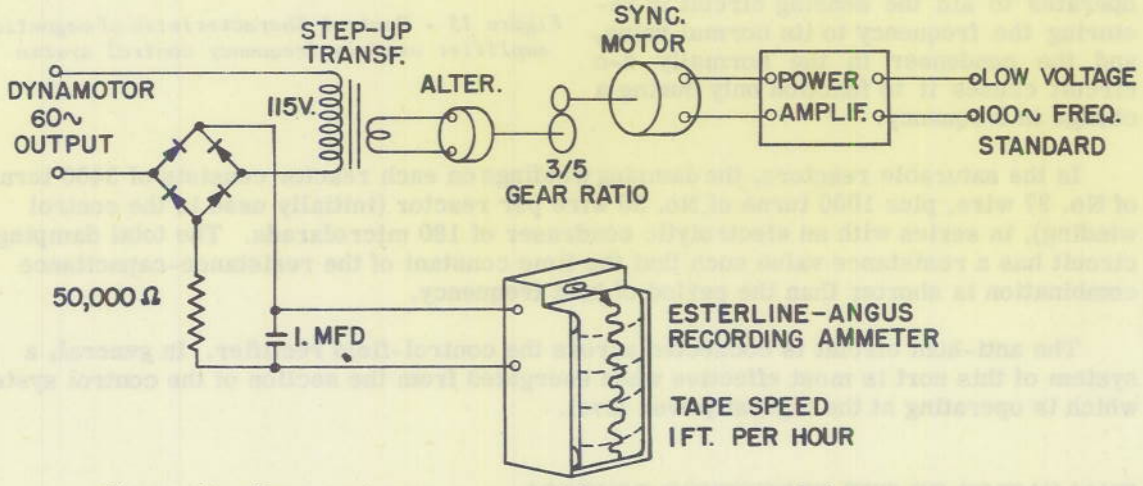

Figure 14 - Test equipment to record frequency error of dynamotor output

The recording instrument in Figure 14 is a direct-current recording milliammeter, so that it is necessary to rectify the input current to the meter. The chart record is interpreted by considering the phase relations between the 60-cycle standard frequency and the dynamotor output frequency which is approximately 60 cycles. When the two voltages to the recorder are exactly in time phase with each other, the current through the recorder is maximum and it indicates a maximum point upscale. When the two voltages are exactly 180° apart in time phase, the current through the milliammeter is a minimum, and the indication of the minimum point is downscale. Minor fluctuations in the line voltages do not appear as errors but are evidenced only by a slight change in the total sweep of the recorder pen, with a slight change in the maximum and minimum values. The chart is driven at a constant rate of one foot per hour and is divided by reference marks for every $2\frac{1}{2}$ minutes of travel. To compute the exact frequency of the dynamotor or the percentage error, it is necessary to count either the number of maximum current peaks recorded or

the number of minimum peaks recorded in a unit of time. If, for example, four peaks are observed during a $2\frac{1}{2}$-minute interval, the error of the dynamotor frequency is 4 cycles in 9000 cycles, or 0.0445 percent. The actual frequency error then is 0.0445 percent of 60 cycles or 0.024 cycles.

In order to determine whether the dynamotor frequency is higher or lower than the standard frequency, a cathode-ray oscilloscope pattern is used. The standard frequency voltage is impressed upon the vertical plates, while the dynamotor output voltage is impressed upon the horizontal plates of the oscilloscope. In this way the direction of rotation of the screen pattern indicates which of the two frequencies is higher.

Evaluation Procedure - Temperature, Voltage, and Load Effects

The general procedure in conducting tests to determine conformance to the specifications consisted of making a series of temperature-cycle runs under every condition of voltage and load on the dynamotor and frequency controller. Over-all performance tests were made with both the dynamotor and the frequency controller inside of the temperature chamber. Temperature-cycling tests were also made with individual components of the system inside of the temperature chamber, but with the other components maintained at room temperature. By means of the latter tests, components having the poorest temperature-stability characteristics were studied and improved. The frequency error of the system was determined under the extreme conditions of voltage, temperature, and load by subjecting the system to a combination of the most detrimental conditions. In the originally designed system, the greatest frequency errors were found to occur at conditions of extreme ambient temperatures, particularly near the high-temperature limit of 130° F.

Evaluation Results

Reactors with Temperature-Stabilized Cores. The toroidal reactors illustrated in Figure 7 were subjected to temperature-cycling tests, both by themselves and in combination with the other components of the frequency-sensing circuits. The results indicate that in the temperature range 40 to 140° F there is practically no measurable frequency error caused by the powdered cores alone (Figure 15).

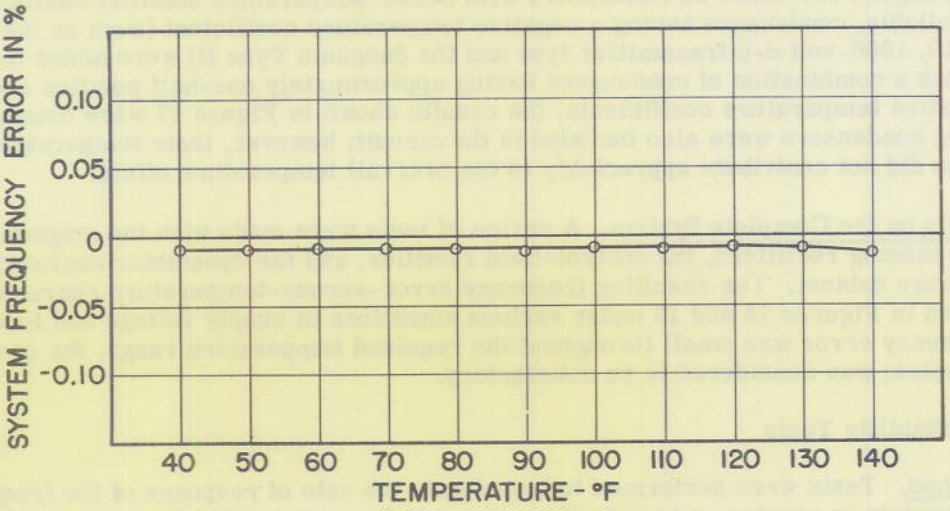

Figure 15 - Temperature characteristics of powdered core reactors

Sensing-Circuit Rectifiers. The original copper oxide rectifiers in the frequency-sensing circuit were found to be unstable with temperature. Results of subjecting the copper oxide rectifiers to various temperatures are shown as frequency-error-versus-temperature curves in Figure 16. By substituting selenium rectifiers (GE type 6RS42F1) for the copper oxide type, the temperature characteristic was improved. Results obtained with selenium rectifiers subjected to a range of temperatures are shown on the same graph with the copper oxide type (Figure 16). The copper oxide rectifiers were not used in this application, but their temperature characteristics are given for comparison.

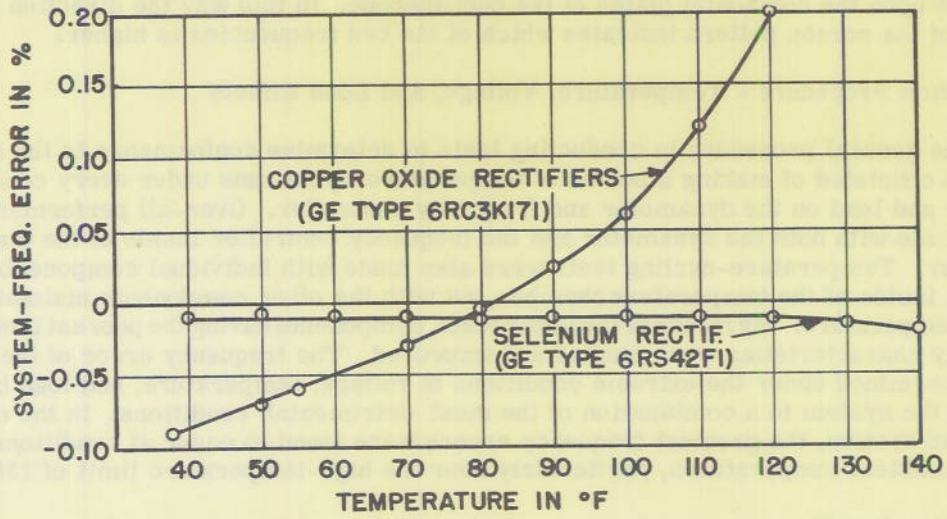

Figure 16 - Temperature characteristics of rectifiers in frequency-sensing circuits

Sensing-Circuit Capacitors. High-voltage condensers (Cornell-Dubilier type 9ALS, 5000 v. dc) were first used in the frequency-sensing circuit. This type of mica condenser, encased in low-loss bakelite, was found to have a positive capacitance drift with increasing temperature. The results of temperature tests for these condensers are shown graphically in Figure 17. Since no condensers with better temperature stability characteristics were available, condensers having a negative temperature coefficient (such as the Illinois type B-10, 1000-volt d-c transmitter type and the Sangamo Type H) were added to the circuit. With a combination of condensers having approximately one-half positive and one-half negative temperature coefficients, the results shown in Figure 17 were obtained. Small trimming condensers were also included in the circuit; however, their temperature coefficients did not contribute appreciably to the over-all temperature effect.

Tests on the Complete System. A series of tests were made with the magnetic amplifier, the biasing rectifiers, the control-field rectifier, and the dynamotor enclosed in the temperature cabinet. The resulting frequency error-versus-temperature characteristics are shown in Figures 18 and 19 under various conditions of supply voltage and load. Since the frequency error was small throughout the required temperature range, the operation of the system was considered to be satisfactory.

Circuit-Stability Tests

Method. Tests were performed to investigate the rate of response of the frequency-control system in sensing and correcting errors in frequency. The time interval and relative change in magnitude of the correcting signal were photographed directly from a d-c cathode-ray oscilloscope set to produce a single sweep across the face of the tube.

Measurements of transient control currents were made, since they directly affect the magnetic-amplifier performance.

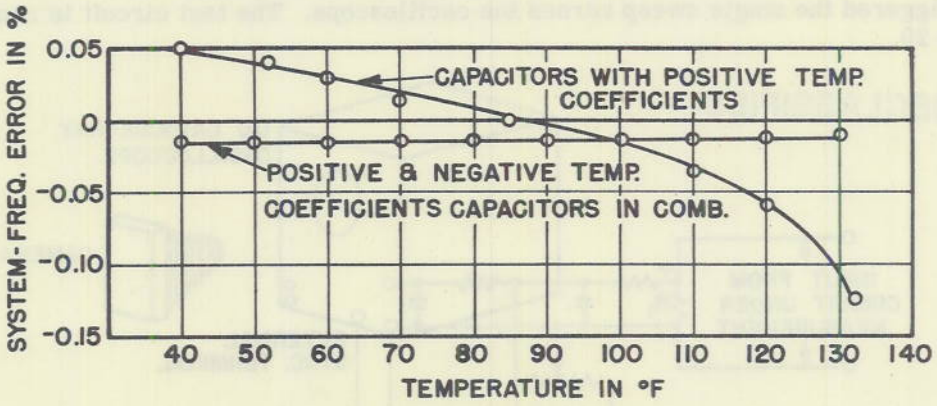

Figure 17 - Temperature characteristics of capacitors in frequency-sensing circuits

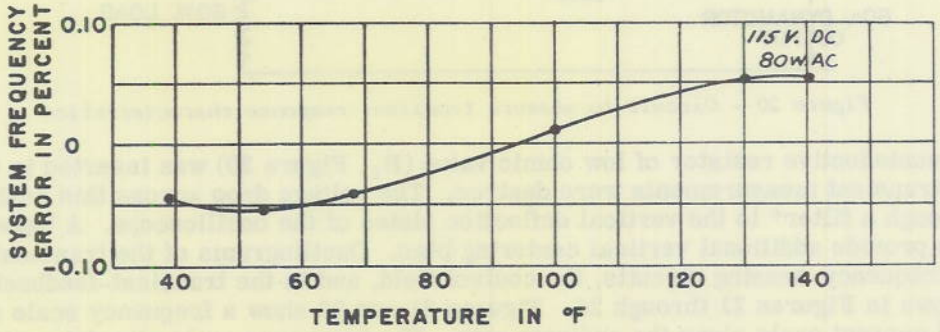

Figure 18 - Over-all temperature characteristic of the magnetic amplifier and dynamotor at normal load and supply voltage

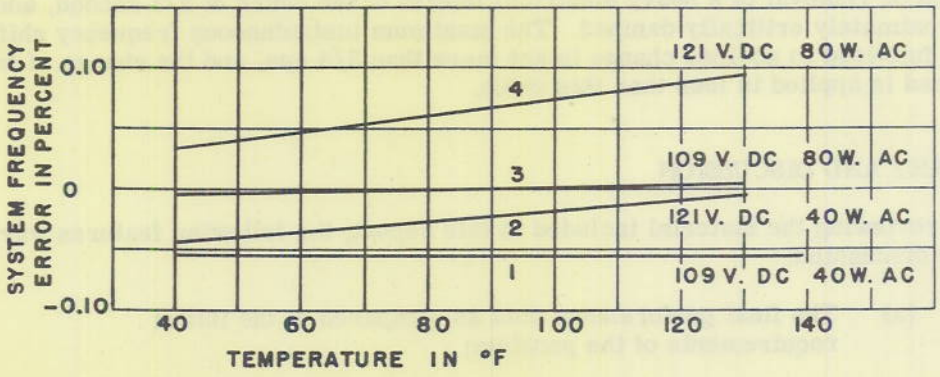

Figure 19 - Performance characteristics of the system under various temperature, load, and supply-voltage conditions

Two different correcting signals were photographed: (1) the transient current produced by suddenly applying a 60-watt resistance load to the unloaded dynamotor, and (2) the transient current produced by suddenly switching off the 60-watt load. The switching operation was performed manually with the test circuit so arranged that the load switch also triggered the single sweep across the oscilloscope. The test circuit is illustrated in Figure 20.

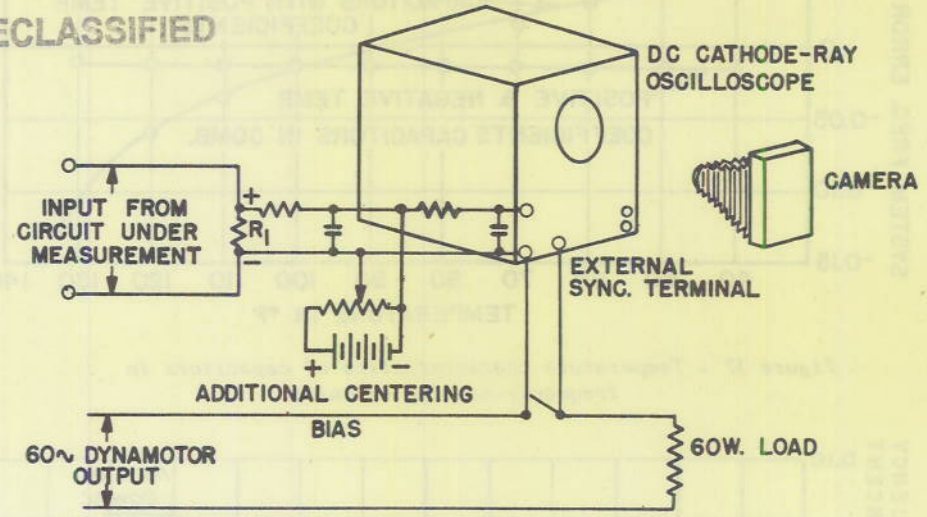

Figure 20 - Circuit to measure transient response characteristics

A noninductive resistor of low ohmic value (R_1, Figure 20) was inserted in the circuit where transient measurements were desired. The voltage drop across this resistor was fed through a filter* to the vertical deflection plates of the oscilloscope. A battery was used to provide additional vertical centering bias. Oscillograms of the transient currents in the frequency-sensing circuits, the control field, and in the transient-feedback winding are shown in Figures 21 through 24. Figures 21 and 22 show a frequency scale and a calibrated current scale along the ordinate axis. The frequency scale was determined from tests on the actual resonant circuits (see Figure 8).

Results. The oscillograms show that the recovery time of the system after the application or removal of a heavy electrical load is of the order of 2/3 second, and the system is approximately critically damped. The maximum instantaneous frequency shift resulting from a full-load to no-load change is not more than 3/4 cps, and the change of frequency when load is applied is less than this value.

SUMMARY AND DISCUSSION

In reviewing the material included in this report, the following features warrant some further discussion:

(a) The final performance data as compared to the initial requirements of the problem;

---

* *Conventional L-pad filters are used to remove ripple-voltage components in the circuit. These voltages contribute nothing towards the control of the machine.*

(b) Other applications of the frequency-regulator circuit;

(c) The determination of optimum core shapes and dimensions.

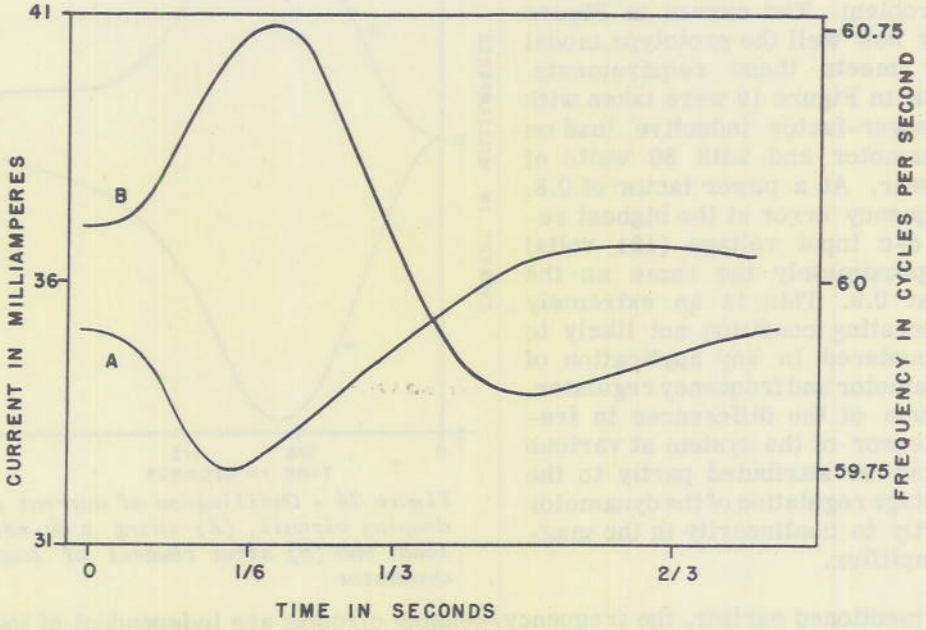

Figure 21 - Oscillogram of rectified current in the 244-cycle frequency-sensing circuit, (A) using a 60-watt a-c load to dynamotor and (B) after removal of load from dynamotor

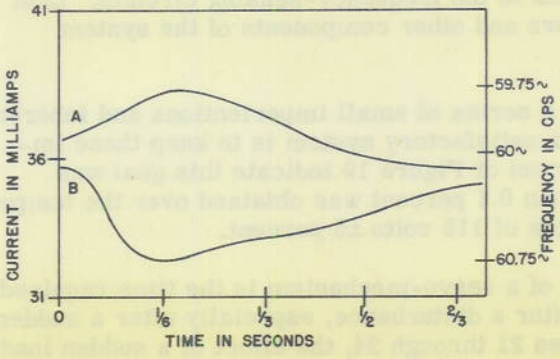

Figure 22 - Oscillogram of rectified current in the 238-cycle frequency-sensing circuit (A) using a 60-watt load to the dynamotor and (B) after removal of load from dynamotor

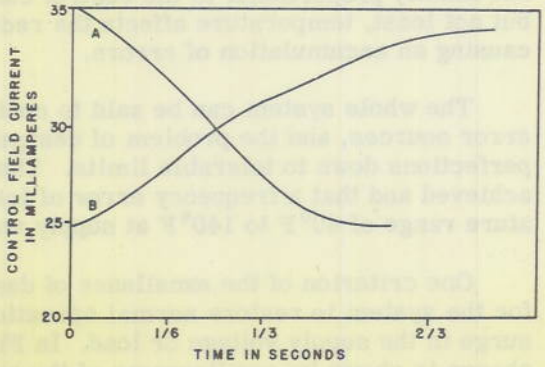

Figure 23 - Oscillogram of transient current in the dynamotor control field, (A) using a 60-watt a-c load to dynamotor and (B) after removal of load from dynamotor

Actual Performance

The introductory paragraphs of this report state the performance requirements to be attained in the development problem. The curves in Figure 19 show how well the prototype model actually meets these requirements. The data in Figure 19 were taken with a 0.9-power-factor inductive load on the dynamotor and with 80 watts of real power. At a power factor of 0.8, the frequency error at the highest required d-c input voltage (121 volts) was approximately the same as the error at 0.9. This is an extremely poor operating condition not likely to be encountered in any application of this dynamotor and frequency regulator. The cause of the differences in frequency error of the system at various loads can be attributed partly to the poor voltage regulation of the dynamotor and partly to nonlinearity in the magnetic amplifier.

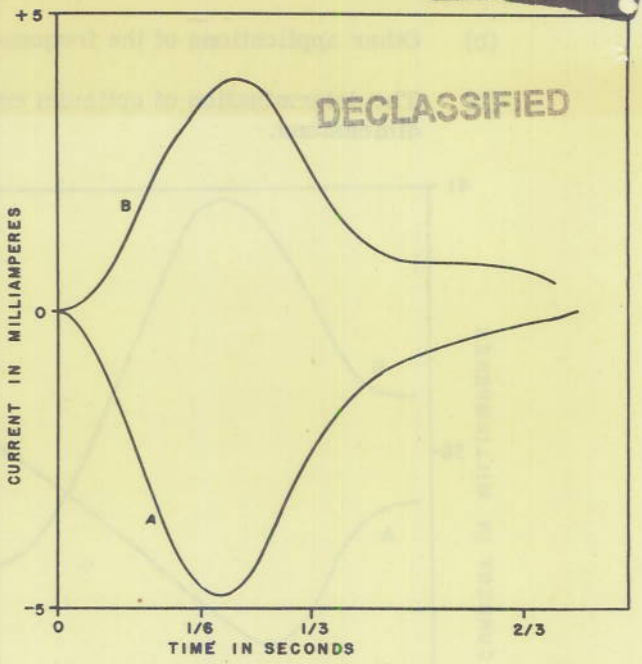

Figure 24 - Oscillogram of current in the damping circuit, (A) using a 60-watt a-c load, and (B) after removal of load from dynamotor

As mentioned earlier, the frequency-sensing circuits are independent of load and power-factor changes. However, the power to the control-field rectifier comes from the a-c side of the dynamotor, and is affected by the a-c regulation, especially near the extreme limits of operating range of the saturable reactors. The magnetic-amplifier reactors are not perfect linear current regulators, and therefore their reactance change is not exactly proportional to the control currents in the frequency-sensing circuits. Last but not least, temperature affects the rectifiers and other components of the system causing an accumulation of errors.

The whole system can be said to contain a series of small imperfections and inherent error sources, and the problem of designing a satisfactory system is to keep these imperfections down to tolerable limits. The curves of Figure 19 indicate this goal was achieved and that a frequency error of less than 0.1 percent was obtained over the temperature range of 40°F to 140°F at supply voltages of 115 volts ±5 percent.

One criterion of the excellence of design of a servo-mechanism is the time required for the system to restore normal operation after a disturbance, especially after a sudden surge in the supply voltage or load. In Figures 21 through 24, the effect of a sudden load change is shown by oscillograms of the currents in the frequency-sensing circuits. The oscillograms show that the system has approximately critical damping, indicating that the sensitivity is near the optimum value.

The common objective in the design of all of the circuit components was to make the operating efficiency high in order to lower the performance requirements of the magnetic amplifier. Examples of the steps taken to relieve the magnetic amplifier of the burden of frequency control in the system are the use of a sensitive control-field winding and a differential compound winding. The differential compound field gives almost complete speed control by itself and is supplemented by the control-field winding, which gives vernier control with only a few watts of power drawn through the magnetic amplifier. Further, to lower

the power-amplification requirements, the sensing circuits are designed to give large changes in control current for small changes in frequency.

The design of a magnetic amplifier having comparatively low sensitivity was dictated by practical considerations, principal among which was the availability of core material for the saturable reactors. It is evident that a servo system having a better distribution of sensitivity between the dynamotor, magnetic amplifier, and frequency-sensing circuits could have been achieved if better reactor core material had been available. A magnetic amplifier having a higher power gain would have made possible a reduction in the Q of the sensing reactors with an improvement in their temperature stability. An amplifier having higher gain and efficiency would also have simplified the problem of designing the dynamotor field winding.

Other Applications

In the course of this development, the magnetic-amplifier frequency control described herein has been applied to a larger motor-generator set having a $1\frac{1}{2}$ horsepower drive motor and a 600 volt-ampere a-c output. The latter machine has performance characteristics superior to those of the smaller dynamotor described previously. Better frequency stability is attained on the larger machine, and the anti-hunt circuit is not needed. The experimental work on a larger machine indicates that extremely low frequency errors could be achieved if an automatic a-c voltage regulator could have been used on the small dynamotor of the original problem. Such a device was not used because the small dynamotor had a common field for both motor and a-c generator.

The magnetic-amplifier principles shown in this report could be applied to voltage regulators as well as frequency regulators. Such devices have been described in the literature.

It appears that the size of the dynamotor or motor-generator set to be regulated is no obstacle to the application of the system described in this report. Much can be done on conventional d-c motors to improve the field-circuit design. If due care is given to the field-coil design, the size of the magnetic amplifier need not increase as rapidly as the power rating of the motor to be controlled. Although no analysis of the power limitations of a one-stage magnetic amplifier has been made in this investigation, it is possible to estimate (from the design values in this report) that a d-c motor of at least five horsepower could be controlled by a one-stage amplifier of reasonable size. For larger machines, a two-stage amplifier would probably be the most satisfactory type to use.

Optimum Cores

An analysis of the optimum core dimensions for a toroidal reactor is given in Appendix 2. So far as is known, this analysis is not in the literature. It is believed that the results of this analysis could be widely used in the interest of obtaining better toroidal reactors of all kinds. It can be shown that the analysis of Appendix 2 is applicable to molded cores of the powdered-metal type. It has been observed that many of the experimental toroidal cores now used in magnetic-amplifier research, as well as in the communications field, have core dimensions far from the optimum values for highest magnetic and electrical efficiencies. It appears that in most cases these experimental cores were designed by empirical methods, whereas a better analytical method can now be used.

CONCLUSIONS

A prototype frequency-control unit of the magnetic-amplifier type has been developed and tested. This model meets the initial problem requirements for accuracy, stability, and

simplicity of construction. If this unit were to be produced in quantity, there would probably be some manufacturing problems still to be solved. However, no serious difficulties in manufacturing or servicing this type of equipment are anticipated. The system is simple and rugged and should give long and satisfactory service with little or no attention in the field.

In the preparation of this report, an attempt was made to supply some specific design information and to outline a method of attack for the solution of a practical problem. It is not intended that this report should be a general treatise on magnetic amplifiers or servomechanisms. The literature is well supplied with papers dealing with the purely theoretical aspects of the subject. There is, however, a pronounced lack of readily usable design information to be found. The theoretical information gathered from literature on the subject was either used or discarded as deemed necessary during the course of the experimental work. Where short-cut methods expedited the solution, they were used without apology, keeping in mind that the purpose of the problem was to design a better frequency-control system with the least possible delay.

It should be emphasized that the design methods are applicable to similar problems as well as to this specific problem. The particular frequency-control unit described here is not important in itself, because it is improbable that the system as it now exists would be duplicated in production. If a quantity of the units were to be built, for example,it would be best to make a new design instead of merely modifying the present one. However, if the design principles described in the report are followed, a wide latitude in the choice of design details can be permitted, with the assurance that satisfactory results will be achieved in the end.

* * *

APPENDIX 1
Performance Data for the Unmodified Dynamotor Unit

In order to redesign the dynamotor unit as a part of the magnetic amplifier frequency control, it was necessary to obtain detailed specifications and performance data on the original machine. This information could have been obtained from the manufacturer, but it was determined as readily by a series of tests.

The specifications for the original unmodified dynamotor were found to be as follows:

Type: Janette type CA-19G
Input: 120 volts dc
Output: 112 volts ac, 60 cycles
Maximum rated current: 3 amperes dc, 1 ampere ac
Output power: 0.08 KVA single phase
Power factor: 0.9 lagging
Number of poles: 2
Speed: 3600 rpm
Temperature rise: 40°C above ambient temperature of 20°C
Field windings: 2 coils of the main field, wound with 1900 turns of No. 30 wire per coil
Resistance of each coil: 220 ohms, corresponding to 2100 feet of wire per coil
Mean length of wire per turn: 1.1 feet.

A cumulative compound field consisting of 20 turns per coil, or a total of 40 turns, was included in the field winding. The circuit of the original dynamotor, along with the winding specifications and a test circuit, are shown in Figure 25. Figures 26 through 28 show the frequency characteristics of the dynamotor at various supply voltage and load values.

The following values also apply to the unmodified dynamotor of Figure 4:

1. Maximum field current for 60-cycle frequency at zero load and 125-volts input: 196 milliamperes

2. Minimum field circuit resistance:

$$\frac{125}{0.196} = 638 \text{ ohms}$$

3. Minimum field current for 60-cycle frequency at maximum load and minimum line voltage (115 watts, 105 volts): 118 milliamperes

4. Maximum field circuit resistance:

$$\frac{105}{0.118} = 890 \text{ ohms}$$

5. Maximum ampere turns for control:

0.196 x 3800 = 746

6. Minimum ampere turns for control:

0.118 x 3800 = 448

7. The difference between maximum and minimum ampere turns is 746 - 448 or 298. These ampere turns must be supplied externally. (The above values are approximate and served only as a guide in designing new field coils.)

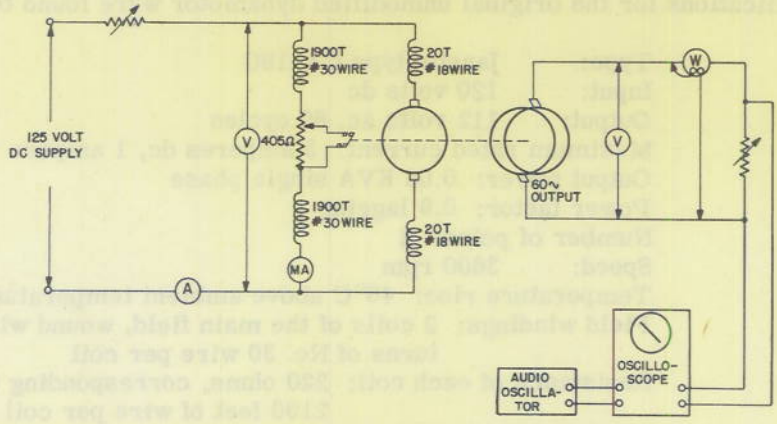

Figure 25 - Circuit used to obtain characteristics of unmodified dynamotor

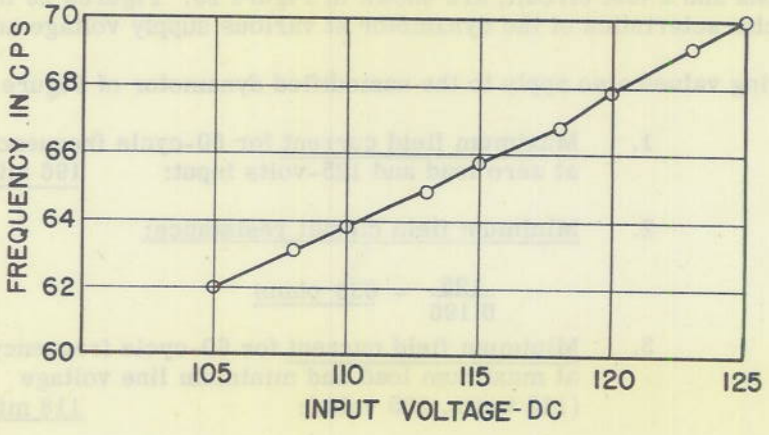

Figure 26 - Frequency vs. input volts constant load of 80 watts a-c output for unmodified dynamotor

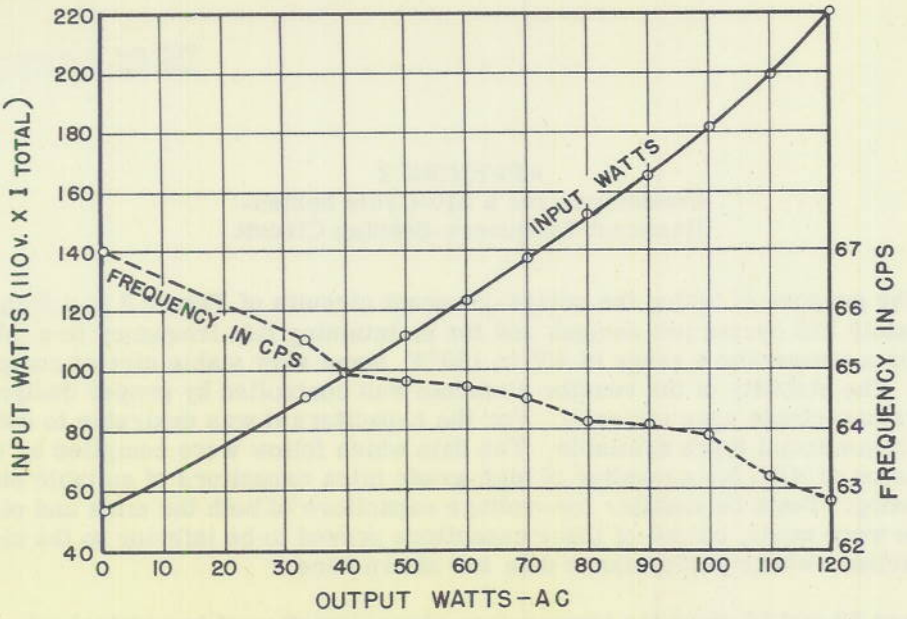

Figure 27 - Frequency and input power vs. load at constant voltage input (110 volts d-c) for unmodified dynamotor

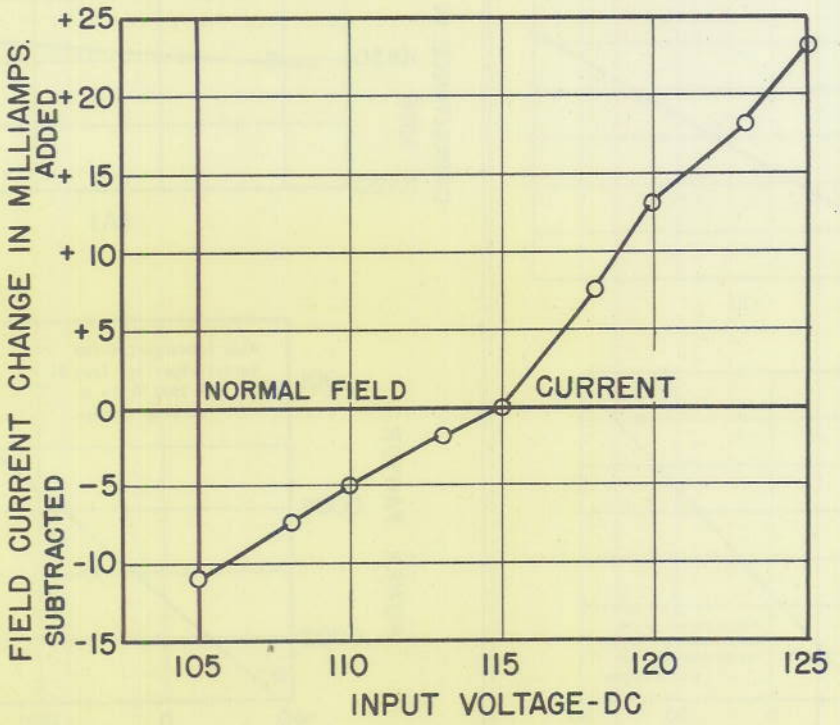

Figure 28 - Field current vs. dc input volts to maintain constant 60 cps frequency

* * *

APPENDIX 2
Condensers for a 240-Cycle Series-Resonant Frequency-Sensing Circuit

For the purpose of tuning the series-resonant circuits of Figure 2 to a frequency of approximately 240 cycles per second, and for maintaining this frequency to a tolerance of ±0.1% over a temperature range of 40° to 130°F, some very stable circuit components were required. The stability of the reactor elements was controlled by proper design and the use of temperature-stable core material. For the capacitors it was desirable to use the best standard commercial types available. The data which follow were compiled by the Chemistry Division of NRL for a number of high-grade mica capacitors of suitable size and voltage rating. Tests on smaller low-voltage capacitors of both the mica and oil-filled paper type were made, but all of these capacitors proved to be inferior to the high-voltage mica capacitors whose performance data are shown here.

Figures 29 and 30 show the temperature characteristics of two typical mica dielectric capacitors used in the frequency-sensing circuits, while Figures 31 and 32 show the temperature characteristics of two other capacitors of similar ratings but of different manufacture.

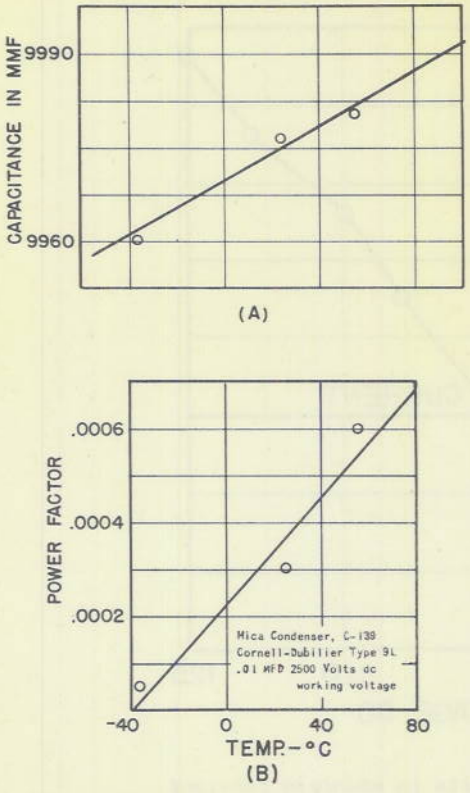

Figure 29 - Temperature characteristic for mica condensers

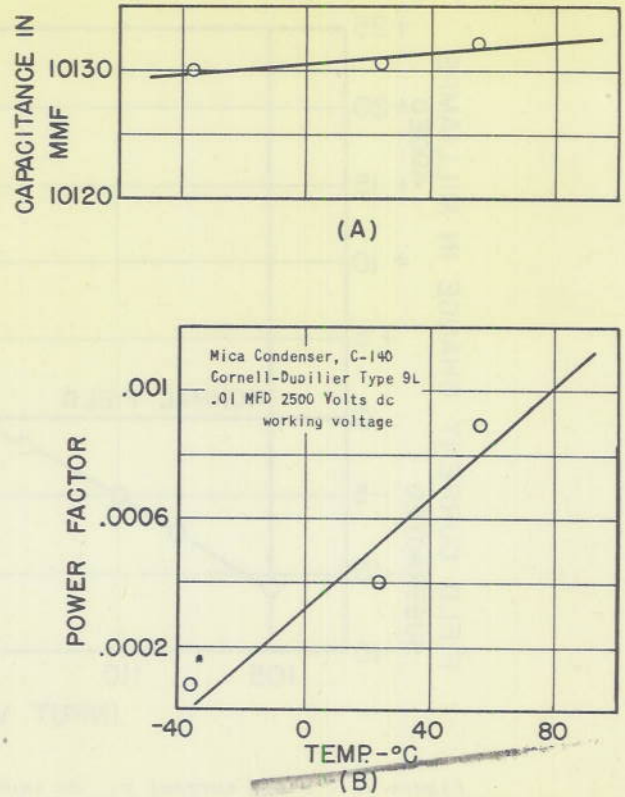

Figure 30 - Temperature characteristic for mica condensers

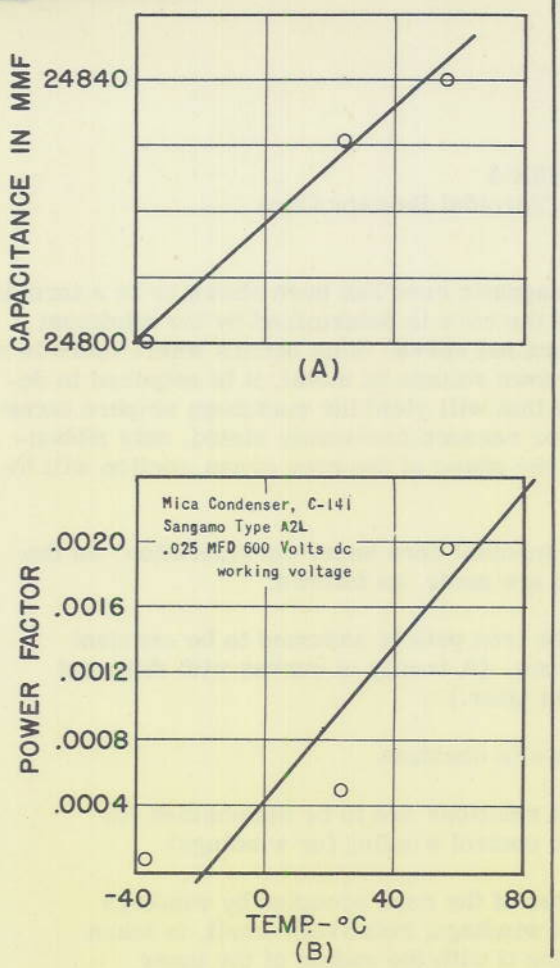

Figure 31 - Temperature characteristic for mica condensers

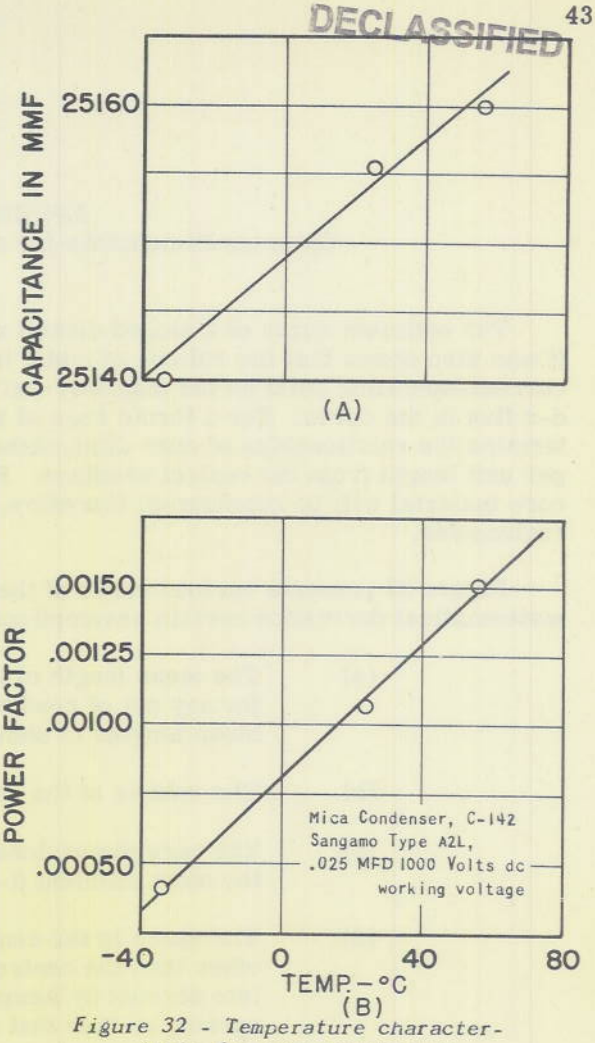

Figure 32 - Temperature characteristic for mica condensers

* * *

APPENDIX 3
Optimum Dimensions for a Toroidal Reactor Core

The optimum shape of a closed circuit magnetic core has been shown to be a toroid. It was also shown that the volume of metal in the core is determined by the minimum current-operating point on the magnetic-saturation curve. This occurs where there is no d-c flux in the cores. For a toroid core of known volume of metal, it is required to determine the relationships of core dimensions that will yield the maximum ampere turns per unit length from the control windings. For reasons previously stated, only ribbon-core material will be considered; therefore, the shape of the core cross section will be rectangular.

Figure 33 presents various views of the toroidal core under consideration. In the mathematical derivation certain assumptions are made, as follows:

(a) The mean length of the iron path is assumed to be constant for any set of conditions. (A family of curves with different mean lengths is shown later.)

(b) The volume of the core is constant.

(c) The core dimensional relations are to be determined for the most efficient d-c control winding (or windings).

(d) The space in the center of the core occupied by windings other than the control windings, relatively small, is taken into account by lumping it with the radius of the inner opening or hole that remains after the windings are in place.

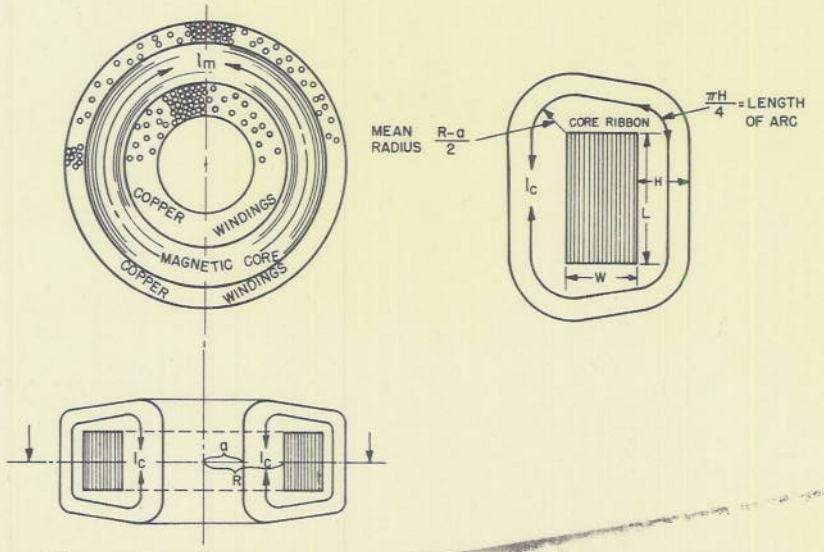

Figure 33 - Toroid type saturable reactor cross sections

From Figure 33, the mean length of copper is

$$l_c = 2L + 2W + \pi\left(\frac{R - a}{2}\right) + \frac{\pi H}{2}, \tag{8}$$

where

V_i = volume of iron

L = length of cross section of iron = $V_i / l_m W$

W = width of cross section of iron

R = inner radius of the core

a = radius of the remaining hole after the winding is in place

H = radial distance from the outside of the core to the outside of the winding

l_m = mean length of iron path.

To obtain an expression for R in terms of l_m and W,

$$R = \frac{l_m}{2\pi} - \frac{W}{2} = \left(\frac{l_m - \pi W}{2\pi}\right). \tag{9}$$

In a toroidal winding, the cross-sectional area of the copper inside of the magnetic core is the same as the copper area outside of the core; therefore, from Figure 33:

$$\pi (R^2 - a^2) = 2\pi \left(R + W + \frac{H}{2}\right) H$$

or

$$H^2 + 2H (R + W) - (R^2 - a^2) = 0. \tag{10}$$

Solving for H,

$$H = -(R + W) \pm \sqrt{(R + W)^2 + (R^2 - a^2)}. \tag{11}$$

Equations (9) and (11) are substituted for the R and H terms in equation (8) to obtain l_c in terms of l_m, R, and W, as follows:

$$l_c = 2(L + W) + \frac{\pi}{2}\left[\left(\frac{l_m - \pi W}{2\pi}\right) - a\right] + \frac{\pi}{4}\left\{-2\left[\left(\frac{l_m - \pi W}{2\pi}\right) + W\right] \pm \right.$$

$$\left. \sqrt{4\left[\left(\frac{l_m - \pi W}{2\pi}\right) + W\right]^2 + 4\left[\left(\frac{l_m - \pi W}{4\pi}\right)^2 - a^2\right]}\right\} \tag{12}$$

Since

$$L = \frac{V_i}{l_m W},$$

$$l_c = \pi \frac{\left[\left(\frac{l_m}{2\pi} - \frac{W}{2}\right) - a\right]}{2} + 2\left(\frac{V_i}{l_m W} + W\right) + \frac{\pi}{2}\left[-\left(\frac{l_m}{2\pi} + \frac{W}{2}\right) \pm \sqrt{\left(\frac{l_m}{2\pi} + \frac{W}{2}\right)^2 + \left[\left(\frac{l_m}{2\pi} - \frac{W}{2}\right)^2 - a^2\right]}\right] \quad (13)$$

The resistance of the control windings, R_c, is

$$R_c = \frac{\rho l_c N}{A_t},$$

where ρ is the coefficient of resistivity and A_t is the cross-sectional area of one turn of wire. Since $A_t = A_c/N$, it follows that

$$R_c = \frac{\rho l_c N^2}{A_c}. \quad (14)$$

The control power, P_c, is the I^2R loss in the control windings; therefore,

$$P_c = I^2 R_c = \frac{\rho l_c N^2 I^2}{A_c} = \frac{\rho l_c}{A_c}(NI)^2. \quad (15)$$

Solving for NI,

$$NI = \sqrt{\frac{A_c P_c}{\rho l_c}}. \quad (16)$$

The area of copper cross section is equal to the area of the core opening less the area of the remaining hole, A_h, after the windings are in place, or

$$A_c = K_c A_h - \pi a^2,$$

or

$$A_c = \pi K_c \left[\left(\frac{l_m}{2\pi} - \frac{W}{2}\right)^2 - a^2\right]. \quad (17)$$

By substituting into equation (16) the expression for A_c from equation (8) and the expression for l_c from equation (13) the following expression for ampere turns per unit length of

magnetic path is obtained:

$$\frac{NI}{l_m} = \sqrt{\frac{P_c K_c \pi \left[\left(\frac{l_m}{2\pi} - \frac{W}{2}\right)^2 - a^2\right]}{\rho l_m^2 \left[\pi\left(\frac{\left[\frac{l_m}{2\pi} - \frac{W}{2}\right] - a}{2}\right) + \frac{2V_i}{l_m W} + 2W + \frac{\pi\left\{-\left(\frac{l_m}{2\pi} + \frac{W}{2}\right) \pm \sqrt{\left(\frac{l_m}{2\pi} + \frac{W}{2}\right)^2 + \left[\left(\frac{l_m}{2\pi} - \frac{W}{2}\right)^2 - a^2\right]}\right\}}{2}\right]}} \quad (18)$$

Equation (18) shows the relationship between ampere turns and core dimensions; however, the control effectiveness is a function of the ratio, NI/l_m. To obtain maximum or minimum values of l_m and W, equation (18) must be either differentiated or plotted. The derivative of equation (18) is a complicated expression; therefore it is found to be more practicable to substitute values in equation (18) and plot curves of NI/l_m versus W.

Several different solutions to equation (18) are found when values of mean length of iron path, l_m, and W are substituted in the equation. In obtaining a set of solutions for equation (18), the following numerical values for the constants were used:

$a = 1$ cm = radius of inner hole of toroid, with windings in place,

$V = 19.22$ cm^3 (assumed to be constant under all conditions)

$K_c = 0.4$ = copper space factor

$\rho = 1.724 \times 10^{-6}$

$P_c = 1$ watt.

Using these constants in equation (18), a solution was found for each of the values of l_m and W shown in Table 4 and plotted in Figure 34.

These results are shown graphically in Figure 30. The values of l_m were chosen by a process of successive approximations. It was known that the cores of Figure 10 (in the text of the report) were not far from the optimum in dimensions. It is to be noted in Figure 34 that the upper curves for l_m in the vicinity of 25 cm tend to converge at the peak value of NI/l_m. Solutions of the equation for other values of l_m cause the peak values of the curves to decrease. The optimum value of l_m can be found by plotting the peak values of each of the curves of Figure 34 as shown in Figure 35.

Thus, from the peak value of the curve of Figure 35, the optimum value of l_m can be determined. In this example, the peak value of lm is approximately 21 cm. Referring back to Figure 34, the value of W can be determined (in this case, approximately 0.7 cm). It is to be remembered that each set of solutions of equation (18) applies to one value of core volume only, as previously determined by the method explained under the section entitled, "Theory and Methods of Design."

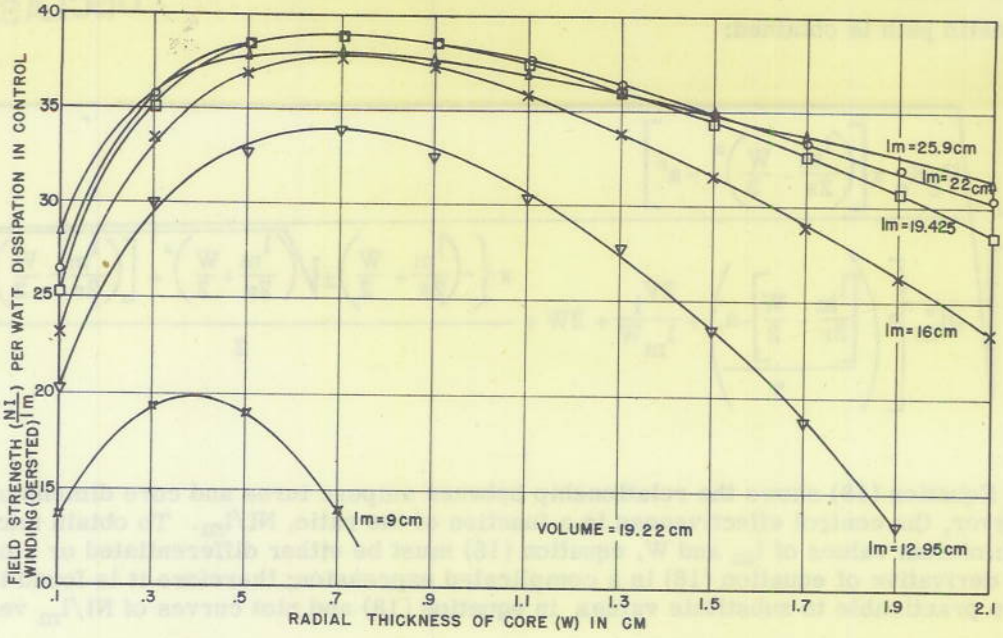

Figure 34 - Optimum dimensional relationships in a toroidal magnetic core

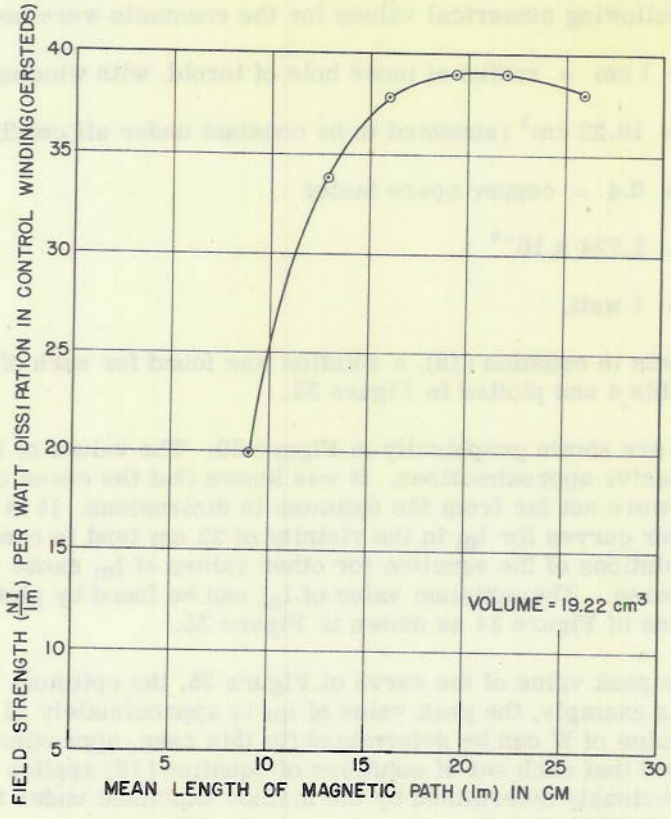

Figure 35 - Optimum dimensional relationships in a toroidal magnetic core

TABLE 4

W	$\frac{NI}{l_m}$ (l_m=9.0)	$\frac{NI}{l_m}$ (l_m=12.95)	$\frac{NI}{l_m}$ (l_m=16.00)	$\frac{NI}{l_m}$ (l_m=19.425)	$\frac{NI}{l_m}$ (l_m+22.0)	$\frac{NI}{l_m}$ (l_m=25.90)
0.1	13.6	20.20	23.2	25.25	--	--
0.3	19.2	30.00	33.5	35.30	35.8	35.80
0.5	19.0	32.80	36.9	38.35	38.4	37.70
0.7	14.0	33.70	37.7	39.00	38.9	38.10
0.9	--	32.50	37.2	38.80	38.5	37.70
1.1	--	30.30	35.7	37.50	37.6	36.90
1.3	--	27.70	33.8	36.10	36.5	36.10
1.5	--	23.50	31.5	34.50	35.1	34.90
1.7	--	19.00	29.1	32.60	33.9	33.80
1.9	--	13.35	26.35	30.90	32.1	----
2.1	--	--	23.5	28.30	30.5	15.05

* * *

APPENDIX 4
Wiring Diagrams for the Saturable Reactors of the Magnetic Amplifier

The schematic diagram of Figure 36 applies to the final model of the magnetic-amplifier frequency control. This figure provides, in addition, a detailed wiring diagram of the magnetic-amplifier unit and the saturable reactors. Figures 37 and 38 are photographs showing constructional details of the magnetic-amplifier frequency control.

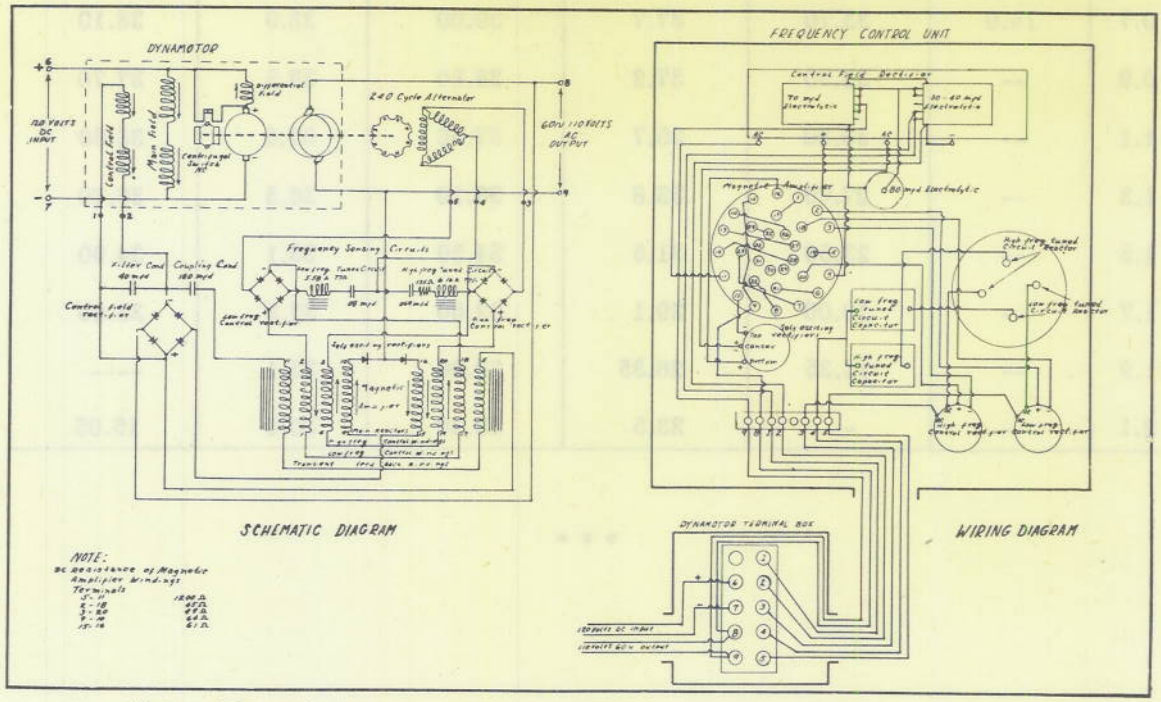

Figure 36 - Schematic and wiring diagrams of frequency control circuit

In an actual installation of this equipment, the color coding of the external cables in Figure 36 must be carefully observed. All external power connections to the system are made in the terminal box of the dynamotor unit.

The schematic diagram of Figure 39 gives the winding data and terminal numbering for the saturable reactors. The saturable reactor used in this design was provided with many more windings and external connections than would be necessary in a production model. However, this frequency-control system is a laboratory model purposely designed for flexibility and ready modification.

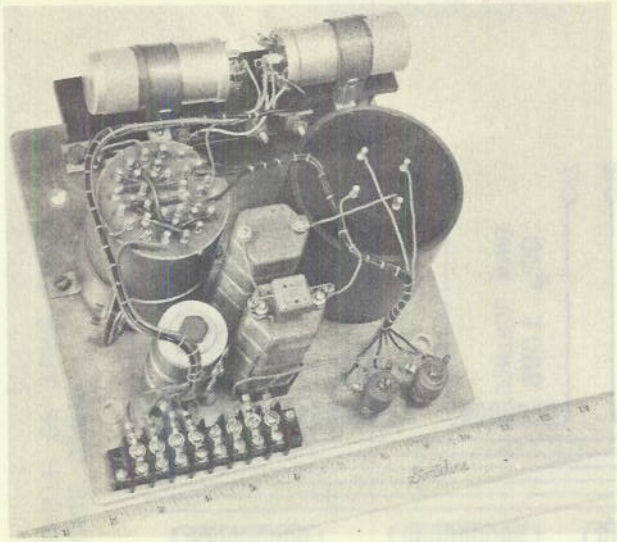

Figure 37 - The frequency-control unit with case removed

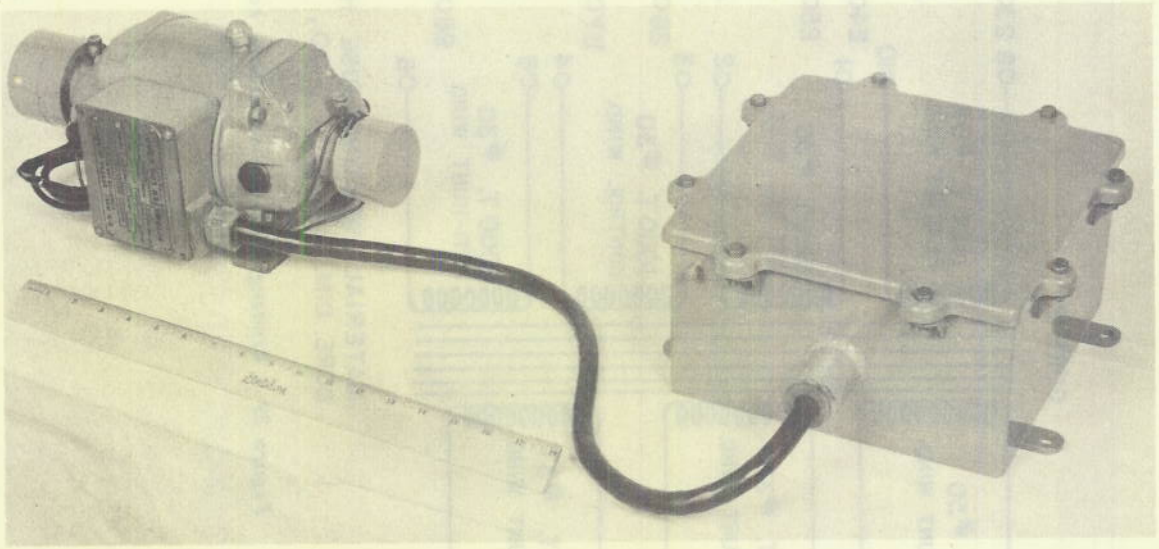

Figure 38 - The frequency-control unit and dynamotor

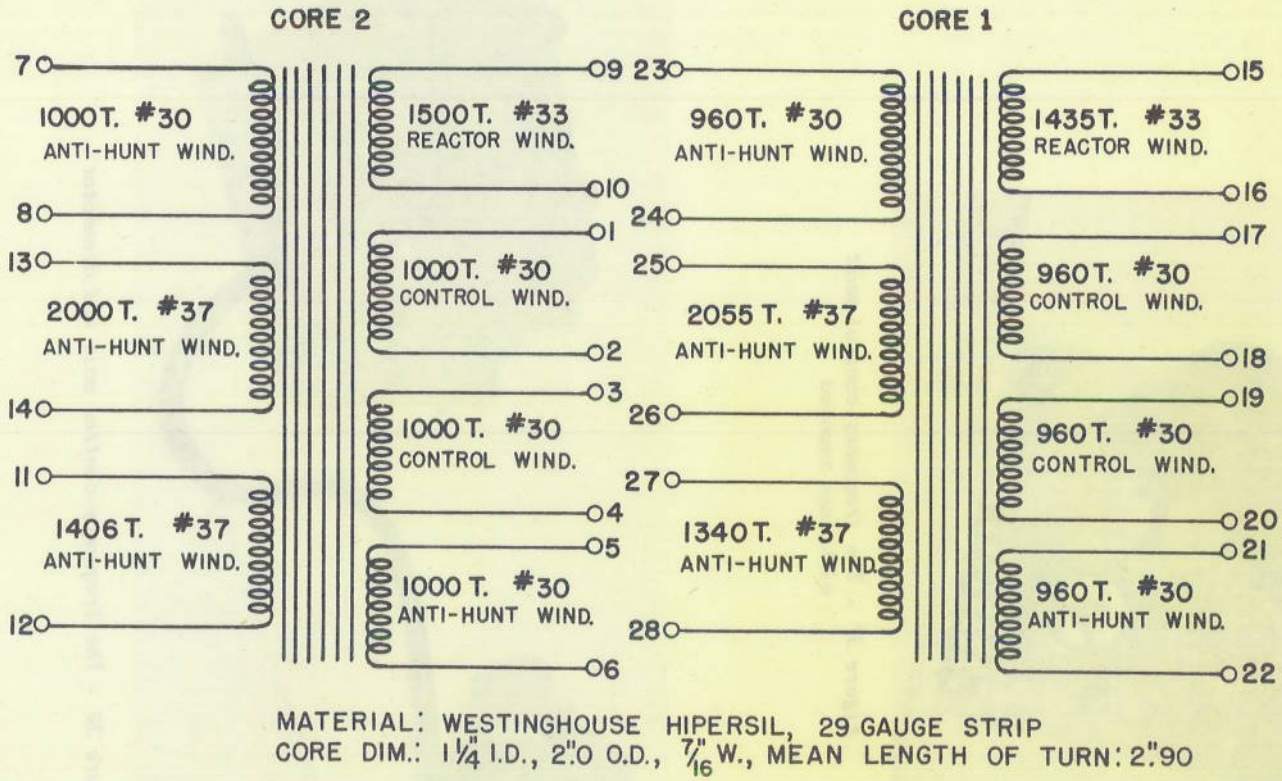

MATERIAL: WESTINGHOUSE HIPERSIL, 29 GAUGE STRIP
CORE DIM.: 1 1/4" I.D., 2".0 O.D., 7/16" W., MEAN LENGTH OF TURN: 2".90

Figure 39 - Winding data for saturable reactors used in magnetic amplifier

BIBLIOGRAPHY

1. Black, A. O., Jr., "Effect of Core Materials on Magnetic Amplifier Design" in Proceedings of the National Electronics Conference, 4: 427-435, 1948

2. Buchhold, T. "On the Theory of Magnetic Amplifiers" Archiv fur Elektrotechnik, 37: 197-211, 1943

3. Elmen, G. W. and Gaugler, E. A. "Special Magnetic Alloys and Their Applications" Electrical Engineering, 67: 843-845, September 1948

4. Holubow, H. "D. C. Saturable Reactors for Control Purposes" Electronic Industries, 4: 76-79, March 1945

5. Lauer, H., Lesnick, R. and Matson, L. E. "Servo-Mechanism Fundamentals" McGraw-Hill, New York, 1947

6. Terman, F. E., "Radio Engineers' Handbook" McGraw-Hill, New York, 1943, pp. 144-145

7. "Papers Presented at the Naval Ordnance Laboratory Magnetic Materials Symposium" NOLR1091. Naval Ordnance Laboratory, White Oak, Maryland, 1 August 1948. Unclassified

8. "Armco Oriented Electrical Steels" American Rolling Mill Company, Middletown, Ohio, 1947

9. "Magnetic Amplifiers" Vickers Electric Division, Vickers, Incorporated, St. Louis, Mo., 1948

NAVY-DPPO PRNC. WASH., D.C.